PL-TR-91-2299

PARAMETERIZED REAL-TIME IONOSPHERIC SPECIFICATION MODEL. PRISM VERSION 1.0

Robert E. Daniell

Computational Physics, Inc.
385 Elliot Street
Newton, MA 02164

1 December 1991

Final Report
15 November 1988 - 15 November 1991

APPROVED FOR PUBLIC RELEASE; DISTRIBUTION UNLIMITED

PHILLIPS LABORATORY
AIR FORCE SYSTEMS COMMAND
HANSCOM AIR FORCE BASE, MASSACHUSETTS 01731-5000

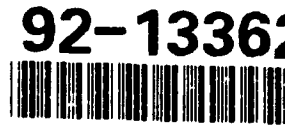

"This technical report has been reviewed and is approved

CHRISTOPHER SHERMAN
Contract Manager

DAVID N. ANDERSON
Branch Chief

FOR THE COMMANDER

WILLIAM K. VICKERY
Division Director

This report has been reviewed by the ESD Public Affairs Office (PA) and is releasable to the National Technical Information Service (NTIS).

Qualified requestors may obtain additional copies from the Defense Technical Information Center. All others should apply to the National Technical Information Service.

If your address has changed, or if you wish to be removed from the mailing list, or if the addressee is no longer employed by our organizati on, please notify GL/IMA, Hanscom AFB, MA 01731. This will assist us in maintaining a current mailing list.

Do not return copies of this report unless contractual obligations or notices on a specific document requires that it be returned.

REPORT DOCUMENTATION PAGE

Form Approved
OMB No 0704-0188

1. AGENCY USE ONLY (Leave blank)	2. REPORT DATE	3. REPORT TYPE AND DATES COVERED
	1 December 1991	Final Report 15 Nov 1988 – 15 Nov 1991

4. TITLE AND SUBTITLE
Parameterized Real-Time Ionospheric Specification Model
PRISM Version 1.0

5. FUNDING NUMBERS
PE 63707F
PR 2688 TA 04 WU JC

Contract F19628-89-C-0005

6. AUTHOR(S)

Robert E. Daniell

7. PERFORMING ORGANIZATION NAME(S) AND ADDRESS(ES)

Computational Physics, Inc.
385 Elliot Street
Newton, MA 02164

8. PERFORMING ORGANIZATION REPORT NUMBER

9. SPONSORING/MONITORING AGENCY NAME(S) AND ADDRESS(ES)

Phillips Laboratory
Hanscom AFB, MA 01731-5000

Contract Manager: Christopher Sherman/GIM

10. SPONSORING/MONITORING AGENCY REPORT NUMBER

PL-TR-91-2299

11. SUPPLEMENTARY NOTES

12a. DISTRIBUTION/AVAILABILITY STATEMENT

APPROVED FOR PUBLIC RELEASE; DISTRIBUTION UNLIMITED

12b. DISTRIBUTION CODE

13. ABSTRACT *(Maximum 200 words)*

This report describes the development of a real-time ionospheric specification model, PRISM, that is based on parameterized physics-based ionospheric models rather than empirical models. PRISM consists of two parts: (1) a database of global ionospheric representations produced by four different ionospheric models developed by Utah State University, the Geophysics Directorate of Phillips Laboratory, and Computational Physics, Inc., and (2) a real-time adjustment algorithm that modifies these ionospheric representations on the basis of ground-based and space-based data. The ionospheric representations in the database are parameterized in terms of Universal Time, season, solar activity, and magnetic activity. The report describes the four physics-based models, the parameterization process, and the real-time adjustment algorithm.

14. SUBJECT TERMS
ionosphere, space environment, ionospheric specification

15. NUMBER OF PAGES
54

16. PRICE CODE

17. SECURITY CLASSIFICATION OF REPORT	18. SECURITY CLASSIFICATION OF THIS PAGE	19. SECURITY CLASSIFICATION OF ABSTRACT	20. LIMITATION OF ABSTRACT
Unclassified	Unclassified	Unclassified	SAR

Table of Contents

Executive Summary

The objective of this program was the development of a truly global near real-time ionospheric specification model (PRISM: Parameterized Real-time Ionospheric Specification Model). PRISM is based on parameterized physical models rather than statistical or climatological models. It uses near real time data from ground based sources (DISS bottomside soundings) and satellite bases sources (DMSP: SSIES in situ plasma measurements, SSJ/4 precipitating ion and electron measurements, and electron density profiles derived from SSUSI and SSULI images) to adjust the parameterized models. Previous specification models were based on a small number of "global" parameters (e.g., effective sunspot number) determined from a limited data set. The adjustment parameters in PRISM vary with location and can be determined from a wide variety of data representing most of the new near real-time data that will become available to the Space Forecast Center during this decade.

Four separate physical models are used in the development of PRISM: a low latitude F layer model, a midlatitude F layer model, a combined low and midlatitude E layer model, and a high latitude E and F layer model. To achieve sufficient computational speed, the models were parameterized in terms of geophysical parameters. The parameterization process involved the production of "databases" for various values of the geophysical parameters and the generation of semi-analytical representations of the databases. The algorithm for adjusting the parameterized models on the basis of real time data is described in this report. The source code, an input data set, and the associated output data stream, all in machine readable form, were delivered to the Air Weather Service at the same time as this report.

Some data has been acquired and more data is being acquired for testing and validating PRISM. Actual validation will begin immediately so that it can be completed before PRISM is released for transition to operational status. A

supplemental report describing the testing and validation process, PRISM performance, and a complete error propagation analysis of PRISM, will be delivered at the same time.

Anticipated future enhancements to PRISM include the use of TISS data and the inclusion of H^+ to extend PRISM to the plasmapause.

Section 1: Introduction

This report describes Version 1.0 of PRISM as delivered to the Air Weather Service. This section describes the development objectives and our approach to achieving them. Section 3 describes the physical models on which PRISM is based. Section 4 describes how the physical models were parameterized. Section 5 describes how the real time data are used to adjust the parameterized model. Section 6 describes the structure of the code, its input and output, and describes the results of some test runs using simulated data. References cited in the text are listed in Section 7.

Section 1.1 Objectives

The primary objective of this effort is the development of an algorithm for using near real time satellite and ground based data to provide a near real time specification of the global ionosphere. The data that are to be used include

(1) bottomside soundings from the DISS network,
(2) Total Electron Content (TEC) data from the TISS network,
(3) in situ plasma data (densities, temperatures, and drift velocities) from the SSIES instrument on DMSP satellites,
(4) auroral electron and ion fluxes from the SSJ/4 instrument on DMSP satellites, and
(5) electron density profile information deduced from the ultraviolet instruments (SSUSI and SSULI) expected to be flown on DMSP satellites.

Unfortunately, complications in making use of TISS data (described below) prevented the use of TISS data in Version 1.0. We anticipate correcting this deficiency in the future. The other four data categories are used in Version 1.0.

The need for a global specification of the state of the ionosphere is twofold. First, there are operational systems that need to correct for ionospheric effects in real time, or that have operational parameters that are affected by the ionosphere and must be adjusted in real time. Further, the operation of these systems could be optimized if accurate forecasts of ionospheric conditions were available because this allows the operational parameters to be chosen ahead of time. Since any ionospheric forecast algorithm will require an accurate specification of the current state of the ionosphere as an initial

condition, this is the second reason an accurate ionospheric specification algorithm is urgently needed.

Section 1.2 Approach

Ideally, the specification of the current state of the ionosphere would be obtained directly from real time observations from a dense network of satellite and ground based instruments. Unfortunately, the complexity of the ionospheric system realistically precludes the deployment of a sufficiently dense network of observing instruments. Therefore, any ionospheric specification algorithm must be based on an ionospheric model with parameters that can be adjusted on the basis of near real time data. Two approaches are possible: (1) statistical or climatological models and (2) numerical simulations based on physical models.

For reasons described below, we have chosen the second approach (physical models). However, practical considerations (primarily computational speed) dictate that the algorithms implemented at the Space Forecast Center be based on *parameterized* versions of the physical models. Thus, we call the global algorithm PRISM for Parameterized Real-time Ionospheric Specification Model.

Section 1.2.1 Motivation

We feel strongly that a comprehensive physical model of ionospheric processes can produce more accurate specifications and forecasts than can statistical or climatological models. The causal relationship between easily monitored solar and geophysical parameters (e.g., K_p, $F_{10.7}$, etc.) and particular ionospheric configuration is very complex. Any organization of historical ionospheric data inevitably averages over a variety of configurations corresponding to similar values of the chosen set of solar-geophysical parameters (usually only one or two). The result is that spatial structure tends to be smeared out or smoothed over and, therefore, unrepresentative of the *instantaneous* ionosphere. If a physical model contains all of the relevant physics, then it will produce more realistic representations of instantaneous ionospheric structure. However, there is a difference between a *realistic* representation and an *accurate* one.

In order to accurately simulate a time dependent phenomenon like the ionosphere, a physical model needs an accurate specification of the initial conditions and an accurate representation of the energy and momentum flux at the boundaries. For the purposes of providing a specification model, it is the energy and momentum input that is crucial. If the model is run long enough, the effects of the initial conditions are lost and the present state of the model depends only on the recent history of the energy and momentum input. These include the solar EUV (the primary source of ionization outside the auroral zone), high latitude heating of the thermosphere (which affects the global circulation of the thermosphere), high latitude convection, and low latitude dynamo electric fields. While the temporal and spatial resolution of the observations of these quantities are expected to improve in the future, they will probably always be insufficient to allow accurate ionospheric simulation of the ionosphere without additional data. As a practical matter, ionospheric simulations must be, and will remain, iterative in nature. The energy and momentum input parameters are adjusted until the simulation agrees with observations of ionospheric parameters to some level of accuracy.

A practical consequence of this situation is that the production of an accurate ionospheric specification based on a numerical simulation requires that the physical model be run several times. The requirement that the model cover a sufficient time period to allow the transient effects of the initial conditions to damp out implies that the physical model must run much faster than the system it is simulating. At the present time, given practical limits on the available computing power, this is not possible. Consequently, we have adopted a modified approach in which the physical models are parameterized in terms of solar and geophysical parameters. It is these parameterized models rather than the original physical models which are to be adjusted according to the real time ionospheric data.

There is a superficial similarity between our approach and a climatological approach. The difference, however, is that we begin with a more realistic representation of the spatial structure of the ionosphere than climatological models can provide. The parameter adjustment process should not compromise this advantage. In the future, as more powerful computers and more efficient model algorithms become available, the parameterized models can be replaced by actual physical models to produce more accurate specifications.

Section 1.2.2 The Parameterization Process

The physical models are parameterized in two steps. First, the physical models are run for a selected set of values of the solar and geophysical parameters (e.g., season, solar activity, and magnetic activity) to produce a set of "databases". Each database consists of ion density profiles for a 24 hour period over the range of latitudes and longitudes for which the model is applicable. Separate models are used for the low, middle, and high latitudes with care taken to ensure smooth transitions at region boundaries. Second, semi-analytical representations of each database are produced. The altitude profiles are represented by linear combinations of Empirical Orthonormal Functions (EOF's, see Section 3.2.1) that are generated for each database. The longitude variation of the coefficients of the EOF's is represented by a truncated Fourier series, and the latitude variation of the Fourier coefficients is represented by a linear combination of orthogonal polynomials (Section 3.2.2). Because the EOF's are tabulated functions, the representation is termed "semi-analytic."

Section 1.2.3 The Real Time Adjustment Algorithm

The semi-analytic representation of each ionospheric "database" allows the results of the physical model runs to be reconstructed quickly and accurately. However, each database corresponds to a specific combination of energy and momentum input conditions, and only rarely will the actual conditions coincide with any one of the databases. Because of the nonlinear nature of the ionosphere, and because each database is represented by a separate set of basis functions (EOF's), the Version 1.0 of PRISM does not interpolate between databases. Instead, the database corresponding most closely to the actual conditions is adjusted on the basis of the available near real time data. The details of the adjustment process are described in Section 4 but will be summarized here. The high latitude region is handled differently than the low and midlatitude regions.

Low and Middle Latitudes. The corrections to the nominal electron density profile will be characterized by eight parameters that are functions of latitude and longitude.

(1) $\Delta f_o F_2$ and (2) $\Delta f_o E$, corrections to the critical frequencies,

(3) $\Delta h_m F_2$ and (4) $\Delta h_m E$, corrections to the heights of the E and F layer peaks,

(5) ΔN_{top} and (6) ΔH_{top}, corrections to the topside electron density and scale height at the DMSP altitude

(7) ΔN_1 and (8) ΔN_2, corrections to the electron density at 8 km and 16 km below the E layer peak, respectively.

These parameters represent a correction to the parameterized model as determined by comparison with near real time data. Thus, the nominal value of each of these parameters is zero, representing no correction to the model.

The F_2 and E layers are separated by composition, i.e., E layer adjustments are affected by adjusting molecular ions (NO^+ and O_2^+) while F_2 layer adjustments are affected by adjusting the atomic ions (presently O^+, but perhaps including H^+ and He^+ in future versions). The critical frequencies (f_oF_2 and f_oE) are adjusted by scaling the appropriate ion density profiles. The layer heights (h_mF_2 and h_mE) are adjusted by shifting the appropriate ion density profiles in altitude. The topside parameters affect only the O^+ (and eventually H^+ and He^+) profiles. The bottomside parameters affect only the molecular ion density profiles. The critical frequencies, layer heights, and the bottomside parameters are determined from DISS data and data from the DMSP UV sensors. The topside parameters are determined from DMSP SSIES and UV sensor data.

The eight adjustment parameters are determined by fitting a simple function of latitude and longitude to the available data. Presently, PRISM uses a simple six parameter function regardless of how much and what kind of real time data is available. However, as we gain experience using PRISM with a variety of data sets, we will experiment with additional parameters to determine the optimal number of parameters under all possible operational conditions.

Because the real time data is not uniformly distributed over the globe, there are always large regions devoid of data. The use of SSUSI images ameliorates this situation somewhat, but does not completely eliminate it. To prevent pathological values of $f(\lambda,\varphi)$ in data starved regions, we introduce "phantom data" from "phantom sites" located in those

regions (Section 4.1). The parameter being fit vanishes at these phantom sites forcing the adjusted ionosphere to "relax" to the model in the data starved regions.

High Latitudes. The previously developed high latitude specification model, HLISM, has been incorporated into PRISM and is used for the trough, auroral, and polar cap ionosphere with a matching algorithm to insure a smooth transition between the midlatitude and high latitude regions. HLISM uses a combination of parameterized physical models and semi-empirical models. Boundaries between the trough, auroral oval, and polar cap regions are determined from DMSP SSIES and SSJ/4 data first. Then the regional models are adjusted using all available data. When they become available, DMSP SSUSI images will be used for both boundary determination and model adjustment. The details of high latitude model adjustment vary depending on the amount and kind of real time data available when the model is run. When data is sparse, the parameterized model is subject to two scalings: first the latitude is rescaled according to K_p, and second a least square adjustment is used to provide an overall adjustment of f_oF_2. When data is abundant, the F layer adjustment makes use of separate f_oF_2 models for each of the three regions (trough, auroral oval, and polar cap). The E layer adjustment uses measured characteristics of precipitating particles (electrons and ions), a parameterized energy deposition model, and a fast local chemistry model to calculate the E layer profile. Initially, precipitation data along the DMSP orbital track will come from SSJ/4, but SSUSI will provide images from which the precipitation parameters can be derived over a large region.

Section 2: The Physical Models

Four separate physical model are used as the basis of PRISM: (1) a low latitude F layer model (LOWLAT), (2) a midlatitude F layer model (MIDLAT), (3) a combined low and middle latitude E layer model (ECSD), and (4) a high latitude E and F layer model (TDIM). (Since the geomagnetic field exerts considerable control over ionospheric phenomena, we use the term latitude to refer to magnetic latitude.) As used to calculate the PRISM databases, all four models use a tilted dipole magnetic field and corresponding magnetic coordinates. All three models use the MSIS-86 neutral atmosphere model [*Hedin*, 1987]. Chemical reaction rates, collision frequencies, and similar data are consistent among all the models.

Section 2.1 The Low Latitude F Layer Model

The low latitude *F* region model (LOWLAT) was originally developed by David N. Anderson [*Anderson*, 1973; reviewed by *Moffett*, 1979]. It solves the diffusion equation for O^+ along a magnetic flux tube. Normally, the entire flux tube is calculated with chemical equilibrium boundary conditions at both feet of the flux tube. A large number of flux tubes must be calculated in order to build up an altitude profile.

Since heat transport is not included, ion and electron temperature models must be used. We chose the model of *Brace and Theis* [1981]. The Horizontal Wind Model (HWM) of *Hedin* [1988] was used to describe thermospheric winds. The critical feature incorporated in the low latitude model is the dynamo electric field. The horizontal component of this field drives upward convection through the **E**×**B** drift, and this can significantly modify profile shapes and densities. This phenomenon is responsible for the equatorial anomaly. The **E**×**B** driven vertical drift used for these calculations was based on data from Jicamarca [*Fejer*, 1981, and *Fejer et al.*, 1989] with modifications to simulate longitude variation.

Section 2.2 The Midlatitude F Layer Model

The midlatitude *F* region model (MIDLAT) is the same as the low latitude version, except that the dynamo electric field is set to zero. Complete flux tubes are followed, but neither horizontal or vertical convection is included. The computer resource requirement of MIDLAT is far less than that of LOWLAT. As long as the boundary between low and middle latitudes is chosen so that the electric field is negligible, the two models should give identical results at the boundary ensuring continuity across the boundary.

Section 2.3 The Low and Midlatitude E Layer Model

The low latitude *E* region model (ECSD) was developed by Dwight T. Decker and John R. Jasperse and incorporates photoelectrons calculated using the continuous slowing down (CSD) approximation [*Jasperse*, 1982]. Ion concentrations are calculated assuming local equilibrium. A small nighttime source is included to ensure a small E layer is maintained during the night.

Section 2.4 The High Latitude Model

The high latitude model (*E* and *F* layers) is the Utah State University (USU) Time Dependent Ionospheric Model (TDIM) developed by R. W. Schunk and J. J. Sojka. [See *Schunk*, 1988 for a review.] This model is similar to the low and middle latitude models except that the flux tubes are truncated and a flux boundary condition is applied at the top. In addition, the flux tubes move under the influence of the high latitude convection electric field. In the low latitudes, because the magnetic field is mainly horizontal, the effect of the electric field is primarily to move the ionization in altitude. In contrast, the high latitude magnetic field is mainly vertical, the electric field driven convection is horizontal.

The TDIM includes an *E*-layer model that incorporates the effects of ionization by precipitating auroral particles. The ion production rates used were calculated using the B3C electron transport code [*Strickland*, 1976; *Strickland et al.*, 1991] and incident electron spectra representative of DMSP SSJ/4 data. The characteristics of the electron spectra were taken from the *Hardy et al.* [1987] electron precipitation model.

Section 3: Parameterization of the Physical Models

Parameterization of the physical models proceeds in two steps. First, the models are used to generate a number of "databases" for a discrete set of geophysical conditions. These databases consist of ion density profiles on a discrete grid of latitudes and longitudes for a 24 hour period in UT. Second, to reduce storage requirements, the databases are approximated with "semi-analytic" functions. These two processes are described in the following subsections.

Section 3.1 Geophysical Parameters

All the physical models have been parameterized in terms of season and solar activity. The middle and high latitude models were also parameterized in terms of magnetic activity, while the high latitude model was additionally parameterized in terms of the sign of the interplanetary magnetic field component B_y. (The high latitude model was only run using B_z southward. Northward B_z conditions are modeled using the low magnetic activity databases.) For the middle and low latitudes, the F layer (O^+) and the E layer (NO^+ and O_2^+) were computed and parameterized separately. The high latitude model (TDIM) produced all three ions simultaneously.

Due to time and computer resource limitations, only a few values of each parameter are used. The season "values" are the June and December solstices and the March equinox (which also "stands in" for the September equinox). The values of the other parameters are summarized for each latitude region in Table 1 on the next page.

Section 3.2 Representation of the Databases

When the models are run for any one set of geophysical parameters (e.g., June, $F_{10.7}$ = 130, K_p = 1), they produce ion densities (O^+, NO^+, O_2^+) on a grid of latitudes, longitudes, and altitudes for a 24 hour period of Universal Time. In order to make this mass of numbers more manageable, we produce a semi-analytical representation of the database. The space and time grid parameters are summarized for each latitude region in Table 2.

Table 1: Geophysical Parameter Values

	Solar Activity $F_{10.7}$	Magnetic Activity K_p	IMF B_y	number of databases
Low Latitude F layer	70, 150, 210	N/A	N/A	36[a]
Midlatitude F layer	70, 150, 210	1, 3.5, 6	N/A	54[b]
Low & Midlatitude E layer	70, 150, 210	1, 3.5, 6	N/A	54[c]
High Latitude E & F layer	70, 130, 210	1, 3.5, 6	+, -	324[d]

[a]3 seasons × 3 solar activities × 4 longitude sectors
[b]3 seasons × 3 solar activities × 3 magnetic activities × 2 hemispheres
[c]3 seasons × 3 solar activities × 3 magnetic activities × 2 species
[d]3 seasons × 3 solar activities × 3 magnetic activities × 2 By's × 3 species × 2 hemispheres

Table 2 Horizontal Grid Parameters

	magnetic latitude	magnetic longitude	UT	number of altitude profiles per database
Low Latitude F layer	-32° to 32° in 2° steps	0°, 30°, 139°, and 237°	0000 to 2330 in 30 min steps	1,584
Midlatitude F layer	30° to 74° and -30° to -74° in 4° steps	0° to 345° in 15° steps	0100 to 2300 in 2 hr steps	3,456
Low and Mid-latitude E layer	-76° to 76° in 4° steps	0° to 345°° in 15° steps	0100 to 2300 in 2 hr steps	11,232
High Latitude E & F layers	51° to 89° and -51° to -89° in 2° steps	7.5° to 352.5° in 15° steps	0100 to 2300 in 2 hr steps	5,760

Due to the computer resource requirements of the low latitude F layer code, it was used to generate databases at four discrete longitudes (corresponding to longitude sectors for which **ExB** drift measurements were available). Each longitude sector was parameterized

separately, and the necessary longitude interpolation is carried out in PRISM during execution.

The parameterization of each database was done in three phases:

Phase 1. Empirical Orthonormal Functions (EOF's) for altitude profiles.

Phase 2. Fourier series for magnetic longitude variation (except low latitude F layer where the UT variation was fit)

Phase 3. Discrete Orthogonal Polynomials for the magnetic latitude variation

Except for the low latitude F layer, all coefficients are tabulated in UT rather than fit with analytic functions. For the low latitude F layer, the UT variation was fit with Fourier series, but the coefficients are tabulated for the four longitude sectors.

Section 3.2.1 *Phase 1*: Empirical Orthonormal Functions

This treatment of empirical orthogonal functions (EOF's) is based on the Appendix of *Secan and Tascione* [1984], which was based on *Lorenz* [1956], *Kutzbach* [1967], and *Davis* [1976]. The reader is referred to these references for mathematical proofs of the assertions made below.

A database consists of altitude profiles at certain longitudes, certain latitudes, and certain Universal Times (Table 2). Let N = the number of altitude profiles in a database, and let M be the number of points in each altitude profile.

We would like to represent each altitude profile of the quantity ψ as an expansion in orthogonal functions, $g_k(z_m)$:

$$\psi_n(z_m) = \sum_{k=1}^{K} \alpha_{nk} g_k(z_m) + r_n(z_m), \qquad n=1...N,\ m=1...M$$

where $r_n(z_m)$ is the residual and the coefficients α_{nk} are calculated from

$$\alpha_{nk} = \sum_{m=1}^{M} \psi_n(z_m)\, g_k(z_m)$$

In principle, any orthogonal set of functions may be used. However, the references provide an algorithm for finding the set which minimizes the RMS error for a given number of terms, K.

First define the M by M covariance matrix C with elements

$$C_{ij} = \frac{1}{N} \sum_{n=1}^{N} \psi_n(z_i)\psi_n(z_j), \qquad i,j = 1,2,...M$$

Now consider the eigenvalue/eigenvector problem $C\phi = \phi L$ or

$$\sum_{j=1}^{M} C_{ij}\phi_{jk} = \sum_{j=1}^{M} \phi_{ij}\delta_{jk}\lambda_k = \phi_{ik}\lambda_k$$

where ϕ is the matrix of eigenvectors of C, and L is a diagonal matrix whose elements are the corresponding eigenvalues. (The k^{th} column of ϕ is the eigenvector corresponding to the k^{th} eigenvalue, λ_k.) By convention, the eigenvectors and eigenvalues are ordered so that $\lambda_1 > \lambda_2 > ... > \lambda_M$. Because C is a real symmetric matrix, eigenvectors corresponding to unique eigenvalues are guaranteed to be orthogonal [See, e.g., *Hildebrand*, 1965]. Because of the origin of the matrix C, it is unlikely that any of its eigenvalues will be degenerate, so we may assume that ϕ is an orthogonal set.

According to *Secan and Tascione* [1984] and references therein, the set of orthogonal functions that minimizes the RMS error for K terms is just the first K eigenvectors:

$$g_k(z_m) = \phi_{mk}, \qquad m=1,2,...M$$

These are the Empirical Orthogonal Functions (EOF's).

As a practical matter, we have found that the number of EOF's needed to provide a reasonably good representation for all the profiles is about $M/6$, as illustrated in Table 3. The only exception is the low and midlatitude E layer (N_2^+ & O_2^+), probably because these databases covered both hemispheres simultaneously. We have also found that substantial improvement in representation does not occur until the number of EOF's is about $M/2$. Furthermore, the EOF's derived for one database were inadequate for any other database, and the EOF's simultaneously derived from several databases produce noticeably poorer representations than those derived for each database individually. Consequently, we have derived separate EOF sets for each database.

Table 3: Altitude Grids and EOF's

Database	number of alt. pts.	minimum altitude	maximum altitude	number of EOF's
low latitude O^+	55	160	1600	9
midlatitude O^+	49	125	1600	8
low & midlatitude N_2^+ & O_2^+	28	90	400	7
high latitude O^+, N_2^+, & O_2^+	37	100	800	6

Note that in none of these cases was the altitude spacing uniform.

The six EOF's derived from the high latitude (USU) database for December, moderate magnetic activity, moderate solar activity, and the BC convection pattern for each of the three ions are shown in Figure 1. The first EOF always has the least structure, and successive EOF's become more structured. The EOF's for low latitude and midlatitude O^+ profiles and for low and midlatitude NO^+ and O_2^+ are shown in Figure 2.

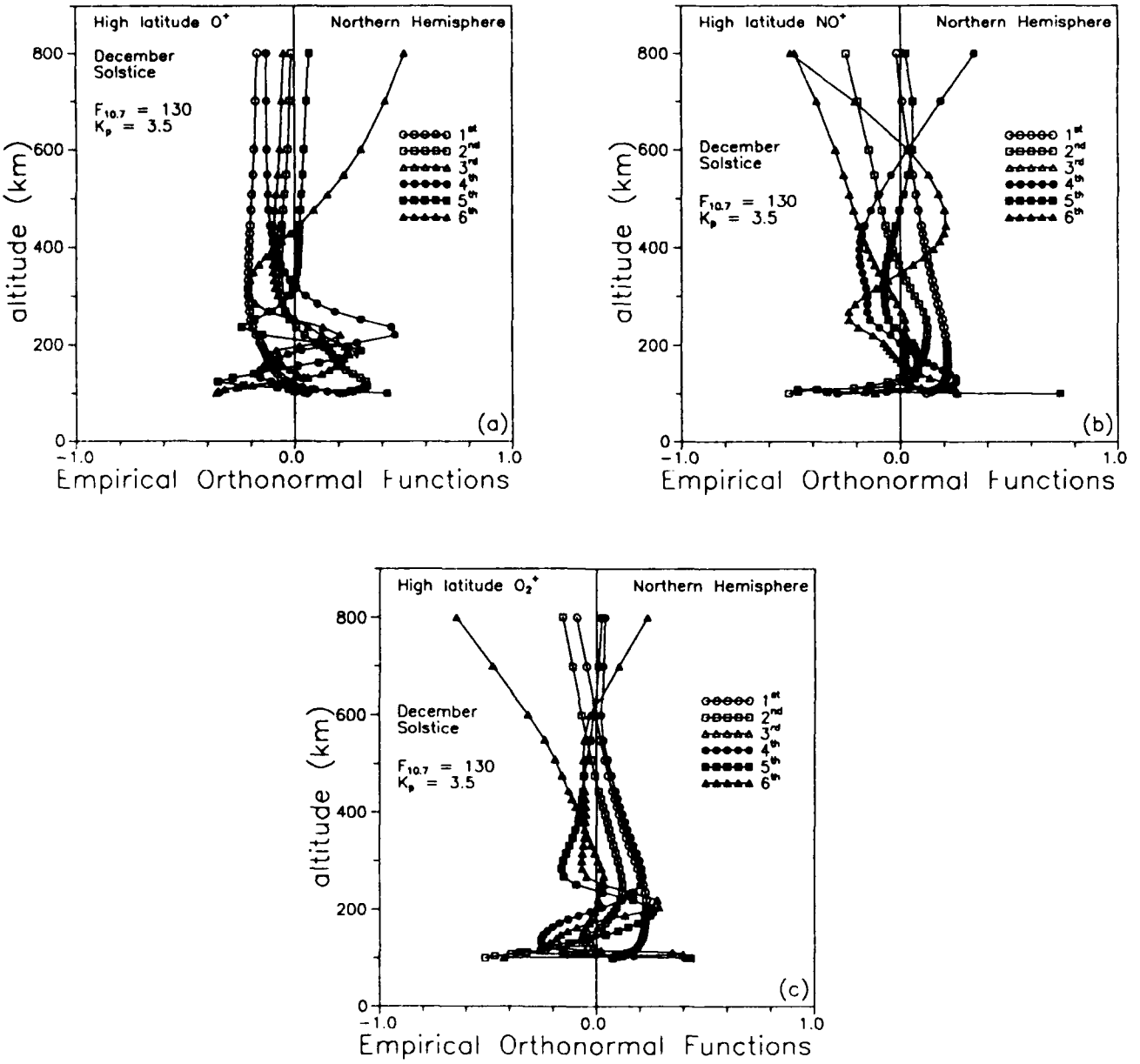

Figure 1: The first six Empirical Orthonormal Functions for (a) O+, (b) NO^+, and (c) O_2^+ derived from the databases for December solstice, moderate magnetic activity, moderate solar activity, and the BC (By>0) Heppner-Maynard convection pattern.

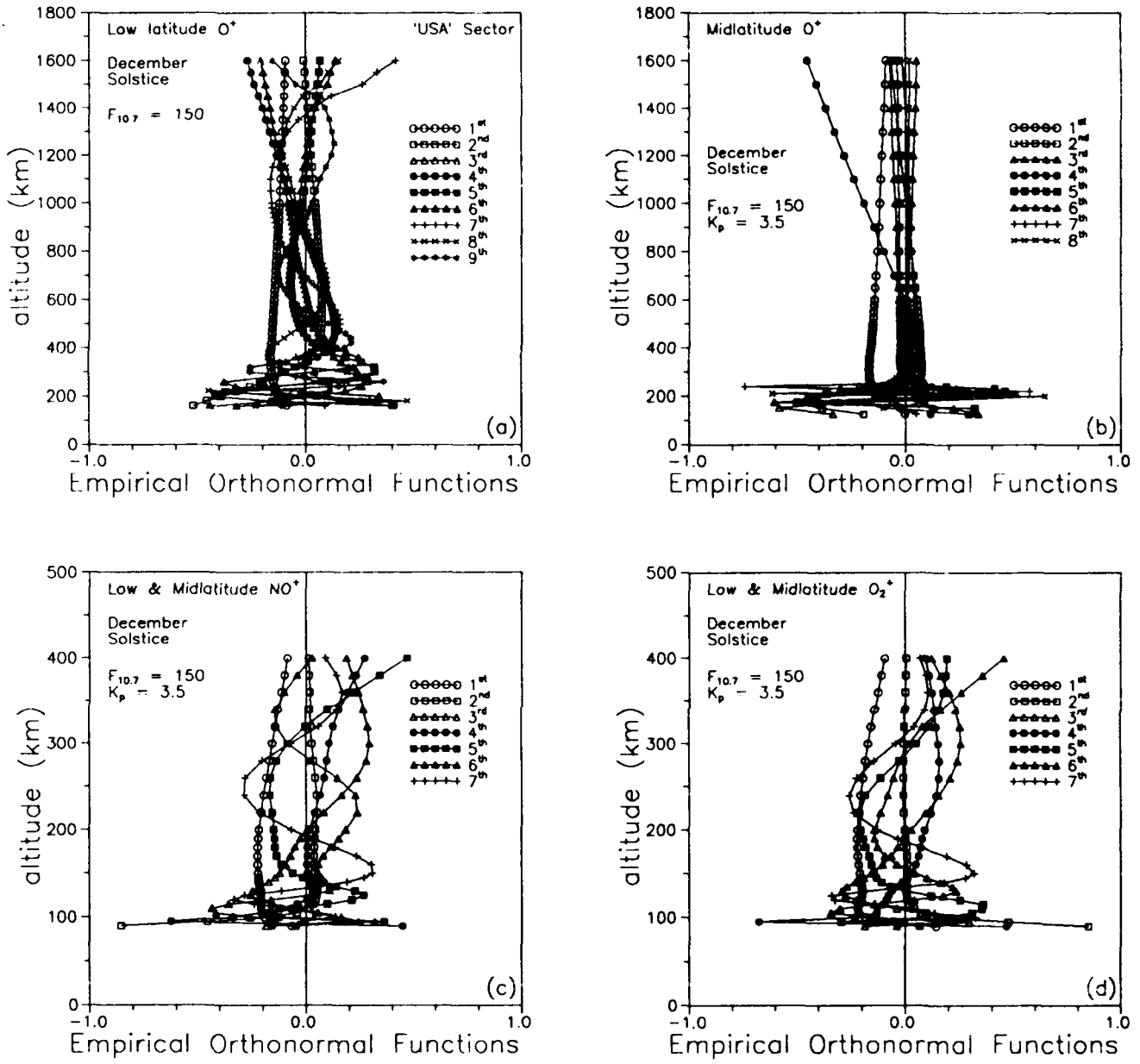

Figure 2: The Empirical Orthonormal Functions (EOF's) for (a) low latitude O^+, (b) midlatitude O^+, (c) low and midlatitude NO^+, and (d) low and midlatitude O_2^+ derived from the databases for December solstice, moderate magnetic activity, and moderate solar activity. For (a) the USA longitude sector is shown.

Section 3.2.2 Local time and latitude representations

Because we were trying to represent discrete data (rather than continuous functions), and because we were working with regional rather than global data sets, we felt that the standard spherical harmonic expansion techniques were not appropriate. Instead, we chose to use orthogonal functions of discrete variables. For longitude variations (and for the low latitude F layer UT variation), the obvious choice was Fourier series, since trigonometric functions retain their orthogonality properties on uniform discrete grids and because the data is periodic in the independent variable. For the latitude variations, we chose to generate orthogonal polynomials using the algorithm derived in *Beckmann* [1973] and described below.

We proceeded in two stages: [1] fit the EOF coefficients, α_{nk}, with Fourier series at each latitude, [2] fit the Fourier coefficients with polynomials in latitude. Recall that the subscript k refers to the EOF while the subscript n refers to a point on the latitude, longitude, UT grid. To make this explicit, let us replace α_{nk} with $\alpha_k(\lambda_p,\varphi_q,t_r)$ where λ is magnetic latitude, φ is magnetic longitude, and τ is Universal Time. Let the number of latitude points be P, the number of longitude points be Q, and the number of Universal Time points be R. Then the total number of points, N, is PQR and the subscript ranges are $1 \le p \le P$, $0 \le q \le Q\text{-}1$, and $0 \le r \le R\text{-}1$. One way of numbering the points is $n = p + qP + rQP$, but any method that assigns a unique number to each point is acceptable.

The Fourier representation of $\alpha_k(\lambda_p,\varphi_q,\tau_r)$ is

$$\alpha_k(\lambda_p,\varphi_q,\tau_r) \approx \frac{\alpha_{k0}}{2} + \sum_{j=1}^{J}\left[a_{kj}(\lambda_p,\tau_r)\cos(j\varphi_q) + h_{kj}(\lambda_p,\tau_r)\sin(j\varphi_q)\right]$$

where

$$a_{kj}(\lambda_p,\tau_r) = \frac{2}{Q}\sum_{q=0}^{Q-1}\alpha_k(\lambda_p,\varphi_q,\tau_r)\cos(j\varphi_q), \qquad j=0,1,\ldots J$$

and

$$b_{kj}(\lambda_p,\tau_r) = \frac{2}{Q}\sum_{q=0}^{Q-1} \alpha_k(\lambda_p,\varphi_q,\tau_r)\,\sin(j\varphi_q), \qquad j=1,2,...J$$

For all of the databases we found that $J = 4$ (giving 9 Fourier coefficients) reproduced the longitude behavior of the α_k's quite well.

The next step was the representation of the a_{kj}'s and b_{kj}'s as functions of magnetic latitude. The algorithm for generating orthogonal polynomials on a specified grid is given by *Beckmann* [1973]. Let us denote the desired polynomials by $u_i(\lambda)$ and define $u_{-1}(\lambda) \equiv 0$ and $u_0(\lambda) \equiv 1$. Let us denote the specified grid by the set of values $\{\lambda_1, \lambda_2, \ldots \lambda_P\}$. The recursion relation for the polynomials is

$$u_{i+1}(\lambda) = (\lambda - B_i)\,u_i(\lambda) - \frac{h_i^2}{h_{i-1}^2}\,u_{i-1}(\lambda)$$

where the norms h_i are given by

$$h_i = \sum_{p=1}^{P} u_i^2(\lambda_p)$$

and the recursion constants B_i are given by

$$B_i = \frac{1}{h_i^2}\sum_{p=1}^{P} \lambda_p u_i(\lambda_p)$$

The polynomials generated by this algorithm may be used to represent the latitude variations of the a_{kj} and b_{kj}:

$$a_{kj}(\lambda_p,\tau_r) \approx \sum_{i=1}^{I} c_{kji}(\tau_r)\, u_i(\tau_p)$$

$$b_{kj}(\lambda_p,\tau_r) \approx \sum_{i=1}^{I} d_{kji}(\tau_r)\, u_i(\tau_p)$$

where

$$c_{kji}(\tau_r) = \frac{1}{h_i^2} \sum_{p=1}^{P} a_{kj}(\lambda_p,\tau_r)\, u_i(\lambda_p)$$

$$d_{kji}(\tau_r) = \frac{1}{h_i^2} \sum_{p=1}^{P} b_{kj}(\lambda_p,\tau_r)\, u_i(\lambda_p)$$

The value of I that gives a good representation of the latitude variation of the Fourier coefficients depends on the number of latitude points in the database grid and the amount of latitude structure in the Fourier coefficients.

low latitude F layer:	$P = 33$	$I = 12$
midlatitude F layer:	$P = 12$	$I = 9$
low & midlatitude E layer:	$P = 39$	$I = 13$
high latitude E & F layer:	$P = 20$	$I = 9$

For most of the databases, the low order c_{kji} and d_{kji} show a simple diurnal variation in Universal Time, but the higher order coefficients show some irregular structure. Consequently, we have chosen not to produce an analytic representation of the UT variation and have simply tabulated the coefficients at the given values.

To reconstruct an O^+ altitude profile in the midlatitude and high latitude F layers, or a molecular ion profile anywhere, one must perform the following steps.

(1) Interpolate the orthogonal polynomial coefficients (c_{kji} and d_{kji}) in UT.
(2) Reconstruct the Fourier coefficients for the desired latitude.
(3) Reconstruct the EOF coefficients for the desired longitude.
(4) Reconstruct the altitude profile from the EOF's.

To reconstruct an O^+ altitude profile in the low latitude region, one must perform a similar sequence of steps.

(1) Reconstruct the Fourier coefficients for the desired latitude for each of the four longitude sectors.
(2) Reconstruct the EOF coefficients for the desired UT for each of the longitude sectors.
(3) Reconstruct the altitude profile for each of the longitude sectors.
(4) Interpolate to obtain the altitude profile at the desired longitude.

The interpolation in step (4) is carried out as a four step process using the following interpolation formula:

(a) Use Fourier interpolation on the f_oF_2 and h_mF_2 values from each longitude sector to obtain the values at the desired longitude.
(b) Scale each profile to match those values (using the algorithms developed for the real time adjustment process and described in Section 4.4).
(c) Use Fourier interpolation on the scaled profiles to obtain an interpolated profile at the desired longitude.
(d) Rescale the interpolated profile to ensure that its f_oF_2 and h_mF_2 match the values obtained in step (a).

The reconstructed profiles are tabulations of concentrations on a discrete altitude grid. Interpolation may be used to obtain concentrations on altitude points lying between grid points.

Section 3.3 Merging the Regional Models

Because we used four different regional models in the development of PRISM, the models must be merged at region boundaries. In particular, the low latitude and midlatitude O^+ models have to be merged across the boundary between low and middle latitudes. All three ions (O^+, NO^+, O_2^+) must be merged across the boundary between midlatitudes and high latitudes.

The transition from low latitude O^+ profiles to midlatitude O^+ profiles takes place between 30° and 34°. The transition is accomplished by taking a weighted average of the h_mF_2 values from the two models in which the weight shifts linearly from 100% low latitude at 30° to 100% midlatitude at 34°. The profiles are shifted to match the averaged h_mF_2 values and then a similar weighted average of the shifted profiles is taken to produce the final merged profile. No transition for NO^+ and O_2^+ is necessary since a single model was used for these ions.

The transition from midlatitude to high latitude takes place over an 8° wide zone whose poleward boundary is the equatorward boundary of the trough. The transition process is similar to the low to midlatitude transition, except that the high latitude profiles are shifted to match the h_mF_2 and h_mE values given by the midlatitude models. The final profile is produced by a weighted average of midlatitude and (shifted) high latitude profiles.

Section 4: Real Time Adjustment Algorithm

The Real Time Adjustment (RTA) algorithm for the low and middle latitude regions is different from the algorithm used in HLISM. This is partly due to the relatively complex morphology of the high latitude ionosphere and partly due to an evolution in our ideas about the real time adjustment process resulting from our experience in developing HLISM.

Section 4.1 Available Data

The near real time data available for use in the adjustment process comes from the Digital Ionospheric Sounding System (DISS), the Transionospheric Sensing System (TISS), and a suite of Special Sensors on the DMSP satellites. These latter include the in situ plasma properties measured by the SSIES instrument, the precipitating particle measurements of the SSJ/4 instrument, remotely sensed electron density profiles (EDP's) from the SSUSI (multispectral UV imager) and SSULI (multispectral limb imager) instruments. The two UV imagers will be flown on DMSP beginning some time in the last half of the decade.

The DISS network consists of about 20 Digisondes located mainly in the northern hemisphere. These digital ionosondes return f_oF_2, f_oE, h_mF_2, h_mE, and parameters that allow the reconstruction of a bottomside profile. The DISS sites (as of 15 June 1990) are shown in Table 4.

The TISS network consists of about 17 suitably equipped GPS receivers located mainly in the northern hemisphere, a number of which are co-located or nearly co-located with DISS sites. The projected TISS sites (as of 9 November 1989) are shown in Table 5. These receivers will provide Total Electron Content (TEC) between the site and the GPS satellites (about 11 earth radii in altitude). When the full constellation of GPS satellites is operational, there will always be at least four satellites in view and sometimes as many as eight. Thus, considerable information about the ionosphere will be produced. Unfortunately, because the quantity provided is an integral quantity (TEC), it is not easy to incorporate it into the PRISM real time scheme. Therefore, we have decided *not* to include TISS data in Version 1.0. However, we have given development of a TISS algorithm first priority for code improvements to be undertaken *after* Version 1.0 has been validated.

Table 4: DISS Sites
(15 June 1990)

site	Name	ICAO	WMO#	lat	lon
a	Amchitka, AK	PAHT	70454	51.38	179.37
b	Argentia, NF	CYAR	71807	47.25	-54.00
c	Bermuda	TXKF	78016	32.37	-64.68
d	Bradshaw AAF, HI	PHSF	91197	19.78	-153.55
e	College, AK	PAEI	70265	64.91	-147.93
f	Diyarbakir, TU	LTCC	17280	37.88	40.18
g	Dyess AFB, TX	KDYS	72266	32.40	-99.86
h	Eglin AFB, FL	KVPS	72221	30.50	-86.50
i	Goose Bay, LB	CYYR	71816	53.32	-60.43
j	Learmonth, AS	APLM	94302	-22.33	114.03
k	Manila, RP	RPMM	98429	14.70	121.10
l	McClellan AFB, CA	KMCC	72483	38.67	-121.40
m	Petersburg, AK	PPSG	70386	56.80	-132.92
n	Osan AB, Korea	RKSO	47122	37.10	127.03
o	Ramey, PR	TJFF	78514	18.50	-67.17
p	Sondrestrom, GL	BGSF	04231	68.00	-51.00
q	Trieste, Italy	LIVT	16110	45.65	13.75
r	Vandenberg AFB, CA	KVBG	72393	34.76	-120.56
s	Wallops Is, VA	KWLI	72402	37.93	-75.47
t	RAF Wethrsfield	EGVT	03688	51.97	0.50

Table 5: TISS sites
(9 November 1989)

site	Name	WMO#	lat	lon	alt (ft)
a	Otis ANGB, MA	72506	41.67	-70.50	130
b	Shemya AFB, AK	70414	52.67	174.17	100
c	Oahu, HI	91182	21.50	-158.00	840
d	Goodfellow AFB, TX	72263	31.33	-100.50	1895
e	Goose Bay, CN	71816	53.33	-60.50	155
f	College, AK	70265	64.83	-147.83	500
g	RAF Croughton, UK	03655	52.00	-1.25	440
h	Thule AB, GL	04205	76.50	-68.75	250
i	Diego Garcia	61967	-7.33	72.42	10
j	Howard AB, PN	78806	8.92	-79.58	50
k	Guam	91217	13.58	144.92	635
l	Churchill, CN	71913	57.50	-94.17	95
m	Keflavik, Iceland	04018	64.00	-22.50	170
n	Ramey, PR	78514	18.50	-67.17	250
o	Beale AFB, CA	72483	39.13	-121.42	115
p	Diyarbakir, TU	17280	37.83	40.17	2250
q	Kunsan AB, ROK	47140	35.92	126.67	50

The DMSP satellites are in approximately circular orbits near 840 km altitude with inclinations chosen to keep the orbit "sun synchronous" – i.e., the local time of the orbit is approximately constant. There are usually two operational satellites at any time, one with an orbit near 0430-1630 local time and the other near 0730-1930 local time. Current satellites carry, among other instruments, the SSIES instrument, which returns ion and electron densities and temperatures, ion drift velocities, and the SSJ/4 instrument, which measures precipitating differential ion and electron fluxes between 20 eV and 20 keV. Beginning near the end of the decade, DMSP satellites will also carry two UV imagers, SSUSI looking down and SSULI looking at the limb. The airglow and auroral optical intensities measured by these two instruments will be used to determine the electron and neutral density profiles. It is not yet clear whether the EDP's will be provided to PRISM, or whether the eight parameters used in PRISM's profile adjustment algorithm will be provided. Either way, PRISM will ultimately use those eight parameters rather than the full EDP's. Initially, each UV instrument will provide EDP's (or EDP parameters) based on its own observations only (single instrument EDP's). However, it is hoped that eventually EDP's will be derived from all four instruments (SSUSI, SSULI, SSIES, and SSJ/4). These should be much more accurate because the data from these instruments is complementary.

Section 4.2 Low and Midlatitude Adjustment Parameters

The RTA will operate on eight parameters that prescribe how an electron density profile is to be modified or "corrected":

(1) $\Delta f_o F_2$, the correction to the model $f_o F_2$, calculated from O^+ profile

(2) $\Delta f_o E$, the correction to the model $f_o E$, calculated from NO^+ and O_2^+ profiles

(3) $\Delta h_m F_2$, the correction to the model $h_m F_2$, calculated from the O^+ profile

(4) $\Delta h_m E$, the correction to the model $h_m E$, calculated from the NO^+ and O_2^+ profiles

(5) ΔN_{top}, the correction to the O^+ density at a specific altitude (i.e., the DMSP altitude)

(6) ΔH_{top}, the correction to the O^+ scale height at a specific altitude (i.e., the DMSP altitude)

(7) ΔN_1, the correction to the electron density 8 km below h_mE, and

(8) ΔN_1, the correction to the electron density 16 km below h_mE.

The nominal value for each of these parameters is zero. A positive (negative) value means that the model value must be increased (decreased). Using the available near real time data, the RTA process will assign non-zero values as functions of magnetic latitude and longitude. The RTA process is described below. The use of the eight parameters to modify the model ion density profiles is described in Section 4.4.

Section 4.3 Real Time Adjustment of the Low and Midlatitude Profile Parameters

In PRISM Version 1.0, Parameters (1), (3), (5), and (7) apply to the O^+ profile only, while the remaining four apply to the molecular ion (NO^+ and O_2^+) profiles only. In either case, the critical frequency and layer height adjustment occurs first, followed by the topside or bottom side adjustment, as appropriate. Each of the eight adjustment parameters are determined by fitting a simple function of latitude and longitude to the available data. The nominal functional form is

$$\begin{aligned} f(\lambda,\varphi) \;=\; & p_1 + p_2\sin\lambda + p_3\cos(2\lambda) + p_4\sin(3\lambda) \\ & + [p_5 + p_6\sin\lambda + p_7\cos(2\lambda) + p_8\sin(3\lambda)]\,\sin\varphi \\ & + [p_9 + p_{10}\sin\lambda + p_{11}\cos(2\lambda) + p_{12}\sin(3\lambda)]\,\cos\varphi \end{aligned}$$

with twelve parameters. When used with data from the 20 station DISS network only, we found it best to set p_6, p_7, p_8, p_{10}, p_{11}, and p_{12} to zero, resulting in a simpler, six

parameter function.

$$f(\lambda,\varphi) = p_1 + p_2\sin\lambda + p_3\cos(2\lambda) + p_4\sin(3\lambda) + p_5\sin\varphi + p_9\cos\varphi$$

When SSUSI data becomes available, potentially providing thousands of EDP's rather than 20, the additional parameters (or perhaps even more) can be used. However, for simplicity and consistency, we have retained the six parameter representation even when using simulated SSUSI data. As we gain experience using PRISM with a variety of simulated data sets, we will determine the optimum parameter set to use with a given complement of data. Due to the modular design of PRISM, it will be easy to upgrade the function fitting algorithm.

Because the real time data is not uniformly distributed over the globe, there are always large regions devoid of data. This is especially true when SSUSI data is absent. To prevent pathological values of $f(\lambda,\varphi)$ in data starved regions, we introduce "phantom data" from "phantom DISS sites" located in those regions. The parameter being fit vanishes at these phantom sites forcing the adjusted ionosphere to "relax" to the model in the data starved regions. (Because the fitting process is a least squares adjustment, the adjustment do not relax exactly to zero, but rather to small values.) The phantom sites are "hard wired" at the locations given in Table 6, which are only used when SSUSI data is absent. So far, we have not found it necessary to use phantom data when SSUSI data is available because the extensive spatial coverage provided by SSUSI images does not leave large areas uncovered. However, we have assumed that SSUSI will provide all eight profile parameters for each complete orbit. It remains to be determined whether or not the SSUSI/SSULI topside parameters for the daytime ionosphere will be sufficiently accurate for use in PRISM.

Section 4.4 Modifying the Low and Midlatitude Model Profiles

The eight parameters will be used to adjust the ion densities profiles in the following ways.

Parameters (1) and (2), the critical frequencies, will be used to scale the entire profile. The F layer (O^+) algorithm is

(a) $N_m F_2 = \max_{0<z<\infty} \left[[O^+](z) \right]$, where $[O^+](z)$ is the O^+ concentration (cm^{-3}) at altitude z,

(b) $f_o F_2(\text{model}) = 8.98 \times 10^{-3} \sqrt{N_m F_2(\text{model})}$, $N_m F_2$ in cm^{-3}, $f_o F_2$ in MHz

(c) $f_o F_2(\text{corrected}) = f_o F_2(\text{model}) + \Delta f_o F_2$

(d) $N_m F_2(\text{corrected}) = 1.24 \times 10^4 \, (f_o F_2)^2$

(e) $[O^+](z,\text{corrected}) = \dfrac{N_m F_2(\text{corrected})}{N_m F_2(\text{model})} [O^+](z,\text{model})$,

and the E layer algorithm is

(a) $N_m E = \max_{0<z<\infty} \left[[NO^+](z) + [O_2^+](z) \right]$, where $[NO^+](z)$ and $[O_2^+](z)$ are the NO^+ and O_2^+ concentrations (cm^{-3}) at altitude z

(b) $f_o E(\text{model}) = 8.98 \times 10^{-3} \sqrt{N_m E(\text{model})}$,

(c) $f_o E(\text{corrected}) = f_o E(\text{model}) + \Delta f_o E$

(d) $N_m E(\text{corrected}) = 1.24 \times 10^4 \, (f_o E)^2$

(e) $$[NO^+](z,\text{corrected}) = \frac{N_m E(\text{corrected})}{N_m E(\text{model})} [NO^+](z,\text{model}),$$

$$[O_2^+](z,\text{corrected}) = \frac{N_m E(\text{corrected})}{N_m E(\text{model})} [O_2^+](z,\text{model}),$$

Parameters (3) and (4), the layer heights, will be used to shift the ion density profiles in altitude. These corrections operate on profiles that have already been corrected according to parameters (1) and (2).

$$[O^+](z,\text{corrected}) = [O^+](z-\Delta h_m F_2,\text{model})$$

$$[NO^+](z,\text{corrected}) = [NO^+](z-\Delta h_m E,\text{model})$$

$$[O_2^+](z,\text{corrected}) = [O_2^+](z-\Delta h_m E,\text{model})$$

Parameters (5) and (6) are used to correct the topside profile based on n_e, n_i, T_e, and T_i measurements from SSIES on DMSP (nominally 840 km). Parameters (7) and (8) are used to correct the bottomside profiles based on bottomside profiles from the DISS network. These four parameters are determined *after* parameters (1) through (4) have been determined, and these corrections are applied to profiles that have already been corrected according to parameters (1) through (4). The topside correction using parameters (5) and (6) follows.

Let $N_m(z)$ be the model O^+ profile (*after* $f_o F_2$ and $h_m F_2$ corrections have been applied). Let $N_c(z)$ be the corrected profile based on ΔN_{top} and ΔH_{top}. Further, let $z_p = h_m F_2$ and z_d = the altitude at which ΔN_{top} and ΔH_{top} were determined. Then define

$$x \equiv \frac{z - z_p}{z_d - z_p}$$

$$y_c(x) \equiv \ln N_c(z)$$

$$y_m(x) \equiv \ln N_m(z)$$

$$g(x) \equiv y_c(x) - y_m(x)$$

so that

$$N_c(z) = N_m(z) \exp[g(x)]$$

Further define

$$R \equiv \ln \left[1 + \frac{\Delta N_{top}}{N_m(z_d)} \right]$$

and

$$S \equiv \left[\frac{1}{H_m(z_d)} - \frac{1}{H_d} \right] (z_d - z_p) = \frac{\Delta H_{top}(z_d - z_p)}{H_m(z_d)\,[H_m(z_d) + \Delta H_{top}]}$$

Determine $g(x)$ from

$$g(x) = \begin{cases} 0, & x < 0 \\ g_1(x), & 0 < x \leq 1 \\ g_2(x), & 1 < x < \infty \end{cases}$$

where $$g_1(x) = (S-2R)x^3 + (3R-S)x^2$$

and $$g_2(x) = Sx + R - S$$

This form ensures that the correction and its first derivative vanish at the peak ($x = 0$), that the concentration and its slope are as specified at z_d ($x = 1$), and that the high altitude behavior of the correction is reasonable.

The bottomside correction proceeds as follows. Let $N_m(z)$ be the model $NO^+ + O_2^+$ profile (*after* f_oE and h_mE corrections have been applied). Let $N_c(z)$ be the corrected profile based on bottomside data. Further, let $z_0 = h_mE$, and let z_1 and z_2 be two altitudes at which the actual electron density has been measured. Then the corrections to $N_m(z)$ at those altitudes are

$$\Delta N_1 = n_e(z_1) - N_m(z)$$

$$\Delta N_2 = n_e(z_2) - N_m(z)$$

For convenience, choose $z_1 = (z_0 + z_2)/2$. Then define

$$x \equiv - \frac{z - z_0}{z_1 - z_0}$$

(Note that x is negative for $-\infty < z < z_0$.)

$$y_c(x) \equiv \ln N_c(z)$$

$$y_m(x) \equiv \ln N_m(z)$$

$$g(x) \equiv y_c(x) - y_m(x)$$

so that

$$N_c(z) = N_m(z) \exp[g(x)]$$

Further define

$$R_1 \equiv \ln \left[1 + \frac{\Delta N_1}{N_m(z_1)} \right]$$

and

$$R_2 \equiv \ln \left[1 + \frac{\Delta N_2}{N_m(z_2)} \right]$$

Let $g(x)$ have the form

$$g(x) = \begin{cases} 0, & x > 0 \\ g_1(x), & -2 \le x \le 0 \\ g_1(-2), & -\infty < x < -2 \end{cases}$$

with $$g_1(x) = (R_1 - \tfrac{1}{2}R_2)x^4 + (4R_1 - \tfrac{7}{4}R_2)x^3 + (4R_1 - \tfrac{5}{4}R_2)x^2$$

This form ensures that the correction and its first derivative vanish at the peak ($x = 0$), that the correction has the desired values at $z = z_1$ and $z = z_2$, and that the correction is well behaved as $z \rightarrow -\infty$.

Section 4.5 The High Latitude Adjustment Algorithm

Due to the complexity of the high latitude ionosphere, the real time adjustment algorithm differs appreciably from the low and midlatitude algorithm. Until SSUSI data becomes available, there will be insufficient data to adjust the parameterized USU model in the way that the parameterized low and midlatitude models can be adjusted. Even with SSUSI data, it is not clear that the midlatitude algorithm is appropriate for the high latitude regions.

In PRISM Version 1.0, the first step in the high latitude real time adjustment process is the establishment of boundary locations. Three boundaries are required: (1) the equatorward edge of the trough, (2) the equatorward edge of the auroral oval, and (3) the equatorward edge of the polar cap.

The equatorward edge of the trough is determined from SSIES drift meter data. The trough boundary as a function of magnetic longitude is given by the formula

$$\theta_t(\varphi) = \theta_0(I_t) + a \exp\left[-\left[\frac{\varphi - b}{c}\right]^p\right]$$

where φ is the magnetic local time (MLT, hours), and I_t is a "trough index" correlated with K_p. $\theta_0(I_t)$ is the radius of the trough boundary at magnetic local midnight and is given by

$$\theta_0(I_t) = 24.4^\circ + 2.12^\circ I_t$$

The second term represents the dayside distortion of the boundary, which would otherwise be a circle centered on the magnetic pole. The parameter values are

$$a = -10.5^\circ$$
$$b = 11.5 \text{ hr}$$

$$c = 3.88 \text{ hr}$$
$$p = 2.73$$

This model is based on the convection boundaries shown in *Heppner and Maynard* [1987].

The equatorward edge of the auroral oval is determined from an analytic representation of the *Gussenhoven et al.* [1983] boundary. The boundary itself is a circle whose center is displaced from the magnetic pole. The radius (in degrees) of the circle is

$$\theta_1(P_1) = 20.9° + 1.7° P_1$$

where P1 is a "precipitation index". The center of the circle is located at

$$\lambda_{c1}(P_1) = 87.3° - 0.267° P_1$$

$$\varphi_{c1}(P_1) = 39.5° - 1.25° P_1 + 0.076° P_1^2$$

where λ_{c1} is magnetic latitude and φ_{c1} is magnetic local time (in degrees).

The equatorward edge of the polar cap has almost the same form, except that it is parameterized in terms of a separate "precipitation index" P_2.

$$\theta_2(P_2) = 13.4° + 1.7° P_2$$

$$\lambda_{c2}(P_2) = \begin{cases} 89.2° + 0.267 \ P_2, & P_2 < 3 \\ 90.8° - 0.267° P_2, & P_2 \geq 3 \end{cases}$$

$$\varphi_{c2}(P_2) = \begin{cases} \varphi_{c1} + 180°, & P_2 < 3 \\ \varphi_{c1}, & P_2 \geq 3 \end{cases}$$

Note that the form of φ_{c2} guarantees that the centers of the two circles lie on a great circle passing through the magnetic pole.

The next step in the high latitude adjustment process depends on the amount and kind of data available. The decision of how to proceed is made separately for the E layer (NO^+ and O_2^+) and the F layer (O^+). In each case, two choices are available:

F layer:

1. Perform a simple least squares adjustment of the USU O^+ model.
2. Use a semi-empirical f_oF_2 model (FMODEL) to adjust the USU O^+ profiles.

E layer:

1. Perform a simple least squares adjustment of the USU NO^+ and O_2^+ models.
2. Use a fast, first principles, E layer local chemistry model (HLE).

The decision is made in PRISM as follows:

data source			model used	
DISS	SSIES	SSJ/4	F layer	E layer
Yes	Yes	Yes	FMODEL	HLE
Yes	Yes	No	FMODEL	USU
Yes	No	Yes	FMODEL	HLE
Yes	No	No	USU	USU
No	Yes	Yes	USU	USU
No	Yes	No	USU	USU
No	No	Yes	USU	USU
No	No	No	USU	USU

In experimenting with high latitude data, we found that extrapolating SSJ/4 data taken along the DMSP orbital track to points well away from the orbital track was very risky. We found no suitable model of the *instantaneous* auroral precipitation for this extrapolation. When SSUSI auroral image data becomes available, this limitation will be removed because much less extrapolation will be required. It should be possible to use HLE whenever timely SSUSI images are available.

FMODEL is a semi-empirical model of f_oF_2 based on a combination of theory and data. It is divided into three regions: the subauroral trough, the auroral oval, and the polar

cap. The f_oF_2 determined by least squares adjustment of the model parameters is used to scale the USU O^+ profiles. No further adjustment of the profiles is performed.

The subauroral trough is divided into two local time regimes: evening (from 1200 to 0000 MLT) and morning (from 0000 to 1200 MLT). Each trough (morning and evening) has a depth parameter that specifies the difference between the midlatitude value of foF2 at the equatorward edge and the trough minimum. The local time variation of the depth is fixed (not part of the least squares adjustment process). If the width of the trough is less than 3°, the depth is reduced in proportion to the width so that when the width vanishes so does the depth. The thickness of the (equatorward) trough wall is always 60% of the total width of the trough. The poleward edge of the trough is the equatorward edge of the auroral F-layer, so the poleward "wall" is considered to be part of the auroral region.

The auroral F layer f_oF_2 is simply a cubic polynomial:

$$f_oF_2(\lambda) = f_{max} + A\,(\lambda - \lambda_{max})^2 + B\,(\lambda - \lambda_{max})^3$$

where $f_{max} = f_oF_2(\lambda_{max})$ is an extremum, and A and B are chosen so that f_oF_2 is continuous across the boundaries with the trough and polar cap:

The background polar cap f_oF_2 is obtained from the URSI coefficients using an effective sunspot number. This is not the same SSNeff used with ICED. Instead, the value of the polar cap effective sunspot number is determined as part of HLISM's least squares adjustment process based on ionosonde data. It should be noted that this part of the model describes only the background polar cap ionosphere.

Section 5: PRISM Execution

PRISM has been delivered to AWS on a DEC TK50 tape cartridge in VAX VMS BACKUP format. Instructions for restoring the files accompanied the tape. The files on the tape cartridge include the complete source code for PRISM, command files for compiling, linking, and executing PRISM, the necessary input and data files for execution, and the output files that resulted when PRISM was executed on CPI/Boston's MicroVAX.

The command file [PRISM.COM_FILES]OPTFOR.COM may be submitted to fully run the code and reproduce the output file that is included on the tape. This command file compiles all the modules and calls OPTLNK.COM. OPTLNK links the modules to produce the executable code. OPTLNK then calls the command file 88113S_UF, which runs the case. As supplied on the tape, this command file requires that PRISM be the main directory, and that the directory structure be as follows.

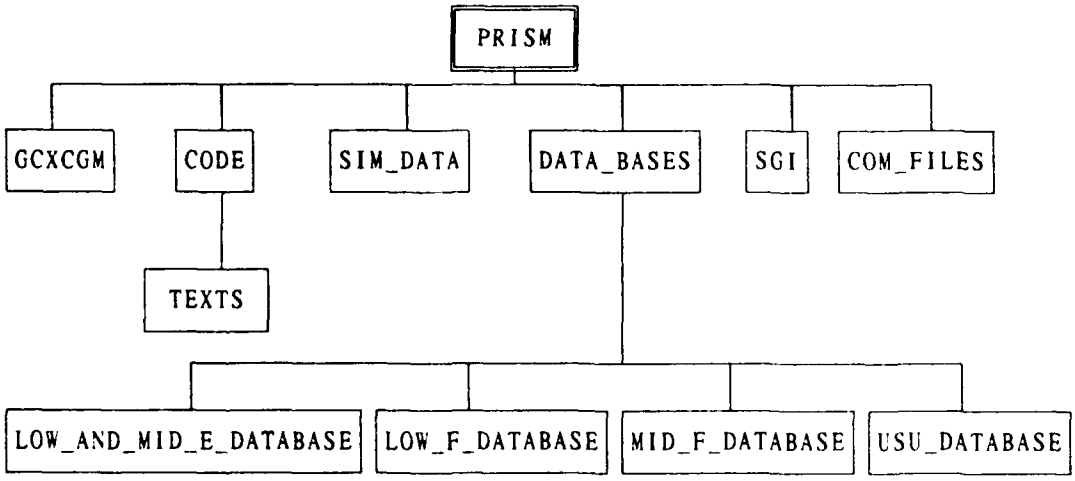

If PRISM cannot be the main directory, or the directory structure cannot be preserved, then the command files must be modified as follows:

If only SIM_DATA, GCXCGM, SGI, or DATABASES is to be changed, then edit the file PATH_NAMES.TXT and give the new directories where the respective data will be.

If the FORTRAN modules of PRISM reside in a different directory, then change OPTFOR, OPTLNK and 88113s_UF to give the correct location of the FORTRAN code.

If PRISM cannot be the main directory, all three command files (OPTFOR, OPTLNK and 88113S_UF must be changed to show the new path to PRISM. PATH_NAMES.TXT must also be changed.

Section 5.1 Code Structure

A complete structure chart for PRISM appears on the following six pages. Because of the complexity of the code, it is broken into major modules. The top level modules are:

GETDAT: which obtains the data used to drive the model, determines boundary locations, and makes certain algorithm choices based on the kind and quantity of data available.

INIT: which initializes various algorithms.

USER_INPUT: which prompts the user for certain choices concerning code operations and reads in the necessary model databases.

MIDLAT: which handles the real time adjustment of the low and midlatitude models.

HLISM: which handles the real time adjustment of the high latitude models.

OUTPUT: which writes the results (EDP's) of the adjustment to a file for subsequent display.

In addition, there are two major modules that service other modules:

REGMOD: which is called by MIDLAT, HLISM, and OUTPUT to produce ion density profiles, scaled and adjusted as necessary, using whichever model is appropriate for the latitude and longitude in question.

HLEMODEL: which is called by REGMOD to calculate the high latitude E layer from first principles when sufficient data is available.

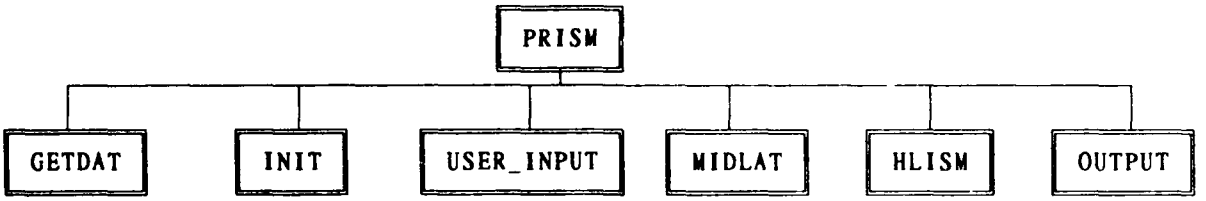
PRISM
GETDAT
INIT
USER_INPUT
MIDLAT
HLISM
OUTPUT

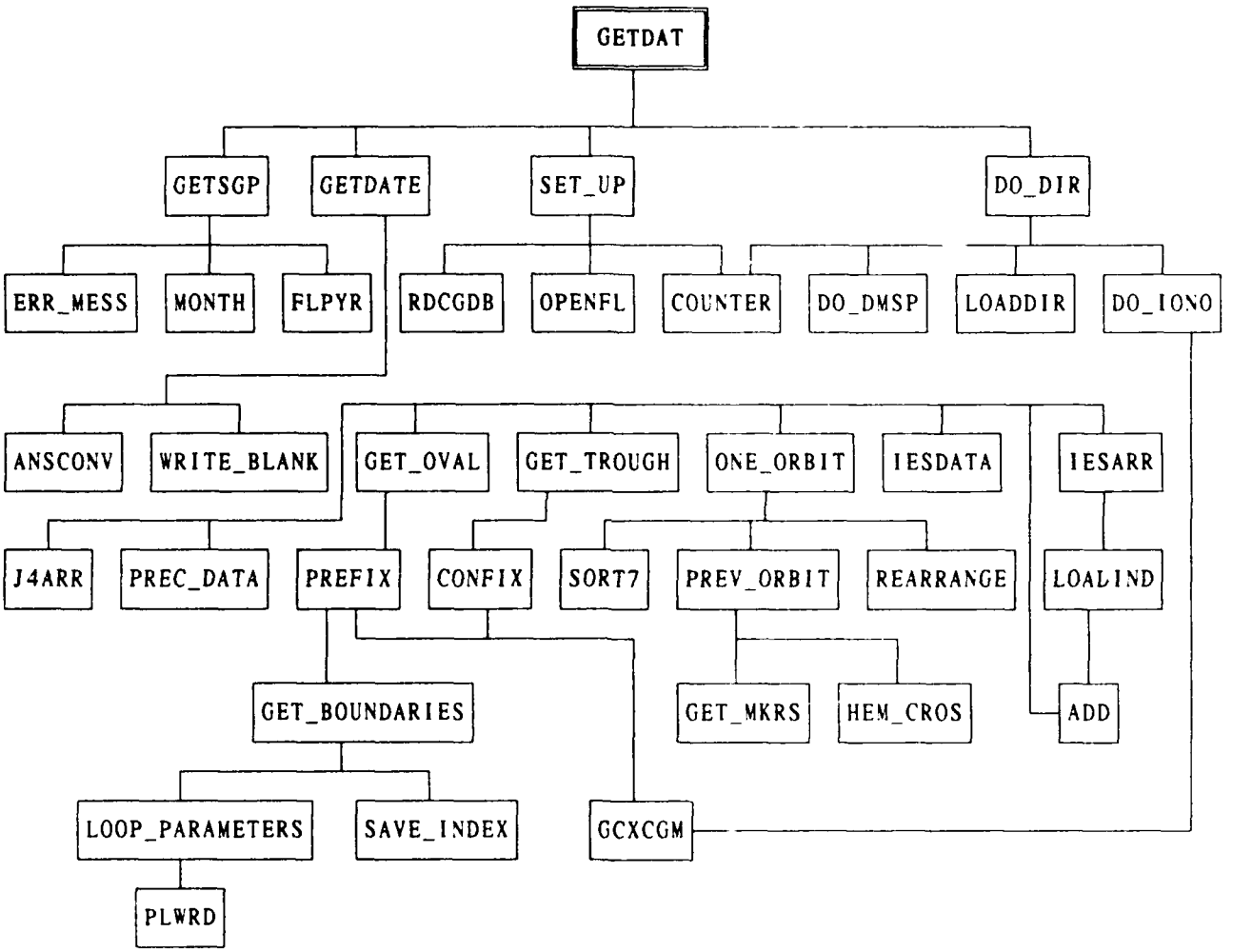
GETDAT
GETSGP
GETDATE
SET_UP
DO_DIR
ERR_MESS
MONTH
FLPYR
RDCGDB
OPENFL
COUNTER
DO_DMSP
LOADDIR
DO_IONO
ANSCONV
WRITE_BLANK
GET_OVAL
GET_TROUGH
ONE_ORBIT
IESDATA
IESARR
J4ARR
PREC_DATA
PREFIX
CONFIX
SORT7
PREV_ORBIT
REARRANGE
LOALIND
GET_BOUNDARIES
GET_MKRS
HEM_CROS
ADD
LOOP_PARAMETERS
SAVE_INDEX
GCXCGM
PLWRD

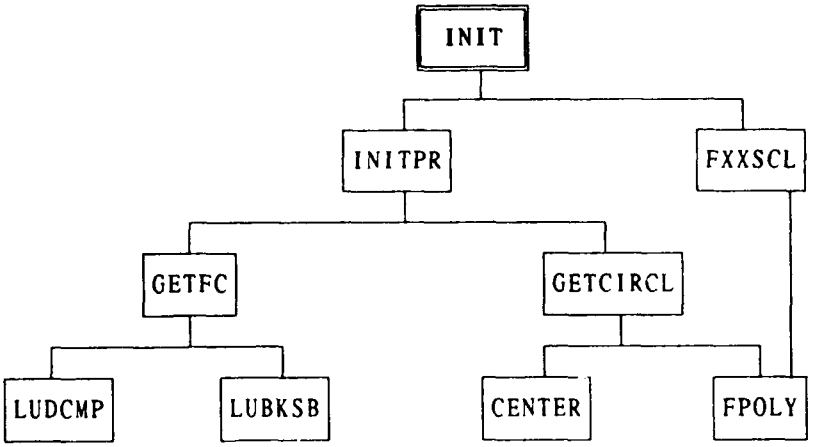
INIT
INITPR
FXXSCL
GETFC
GETCIRCL
LUDCMP
LUBKSB
CENTER
FPOLY

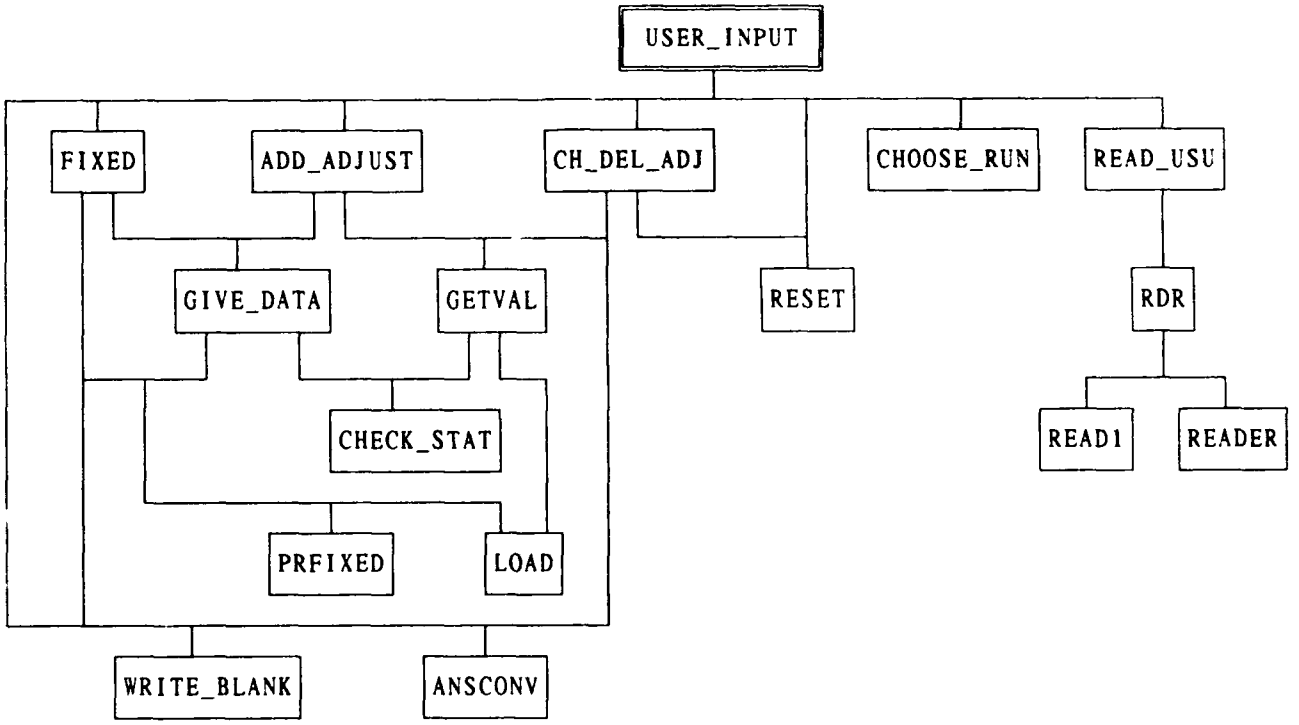
USER_INPUT
FIXED
ADD_ADJUST
CH_DEL_ADJ
CHOOSE_RUN
READ_USU
GIVE_DATA
GETVAL
RESET
RDR
CHECK_STAT
READ1
READER
PRFIXED
LOAD
WRITE_BLANK
ANSCONV

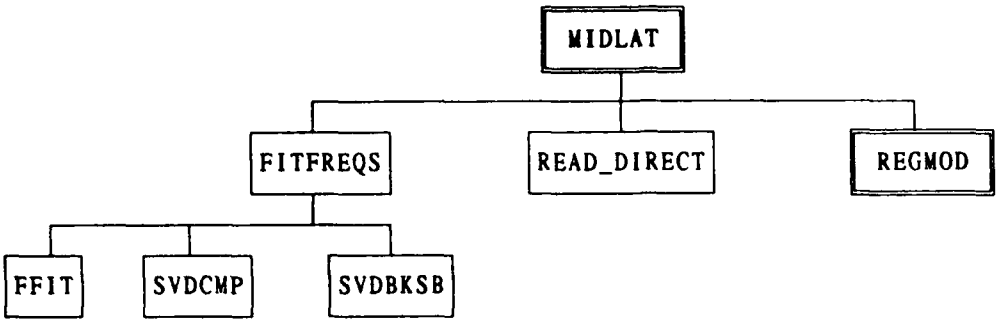
MIDLAT
FITFREQS
READ_DIRECT
REGMOD
FFIT
SVDCMP
SVDBKSB

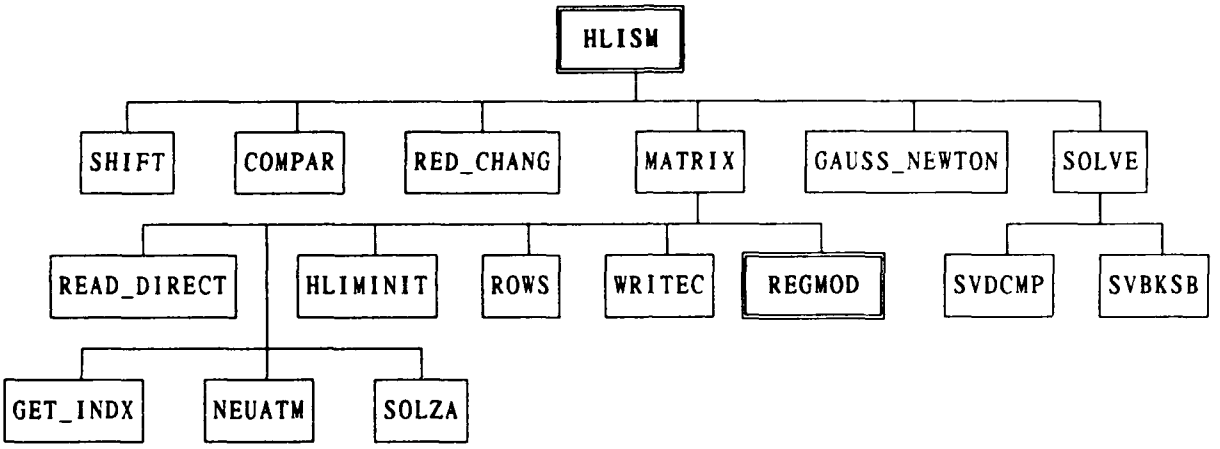
HLISM
SHIFT
COMPAR
RED_CHANG
MATRIX
GAUSS_NEWTON
SOLVE
READ_DIRECT
HLIMINIT
ROWS
WRITEC
REGMOD
SVDCMP
SVBKSB
GET_INDX
NEUATM
SOLZA

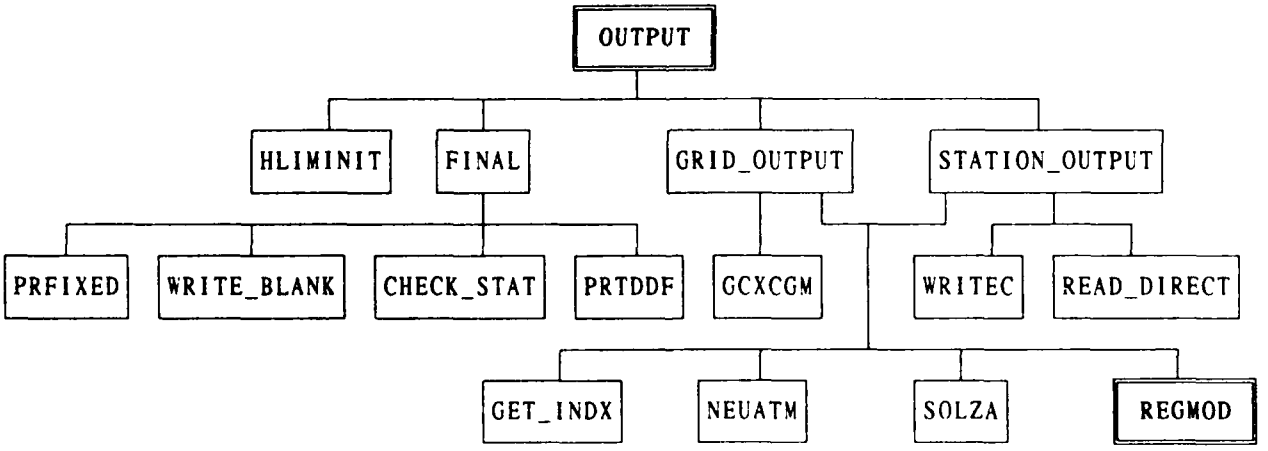
OUTPUT
HLIMINIT
FINAL
GRID_OUTPUT
STATION_OUTPUT
PRFIXED
WRITE_BLANK
CHECK_STAT
PRTDDF
GCXCGM
WRITEC
READ_DIRECT
GET_INDX
NEUATM
SOLZA
REGMOD

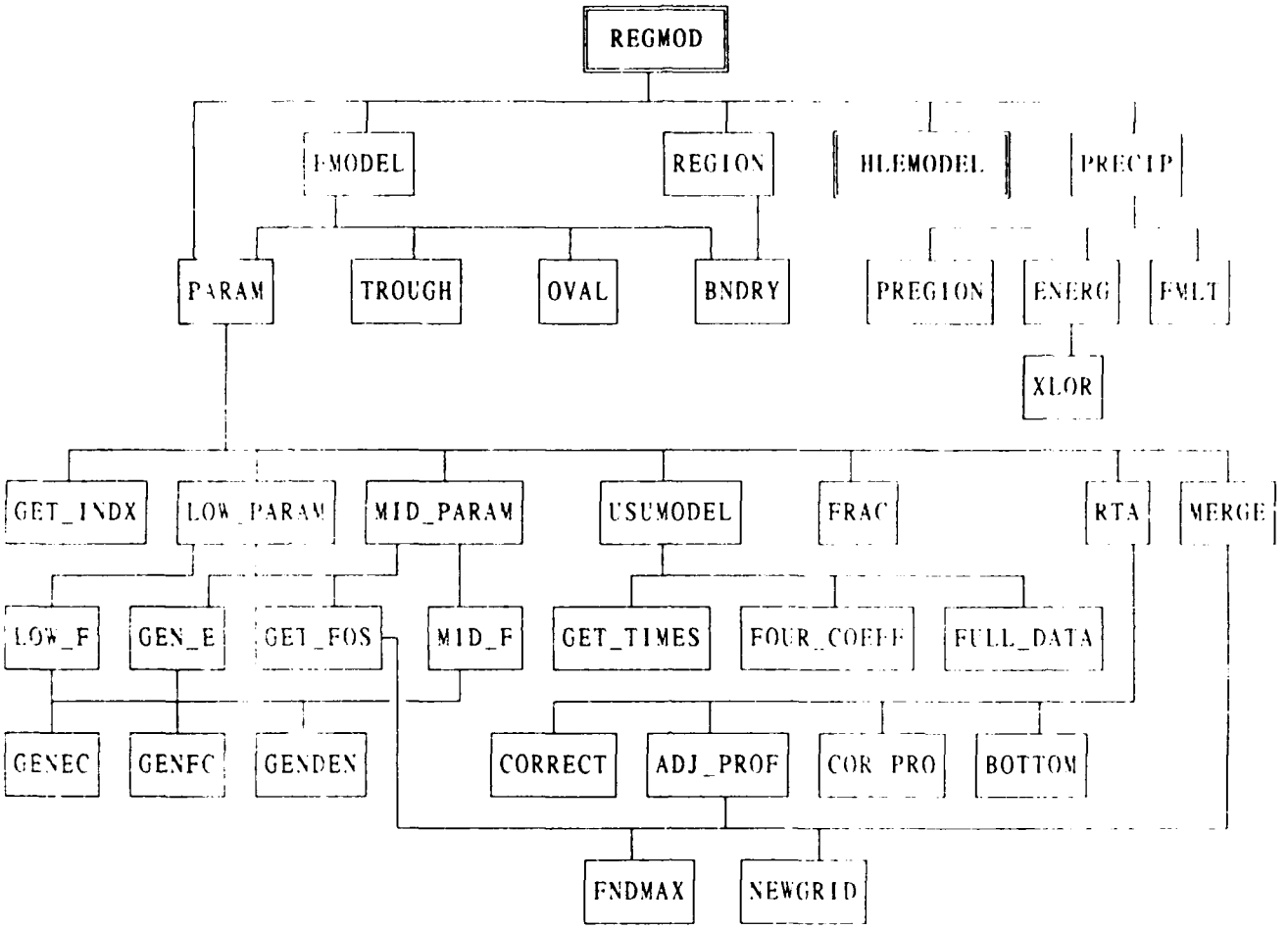
REGMOD
F-MODEL
REGION
HLEMODEL
PRECIP
PARAM
TROUGH
OVAL
BNDRY
PREGION
ENERG
FMLT
XLOR
GET_INDX
LOW_PARAM
MID_PARAM
USUMODEL
FRAC
RTA
MERGE
LOW_F
GEN_E
GET_FOS
MID_F
GET_TIMES
FOUR_COEFF
FULL_DATA
GENEC
GENFC
GENDEN
CORRECT
ADJ_PROF
COR_PRO
BOTTOM
FNDMAX
NEWGRID

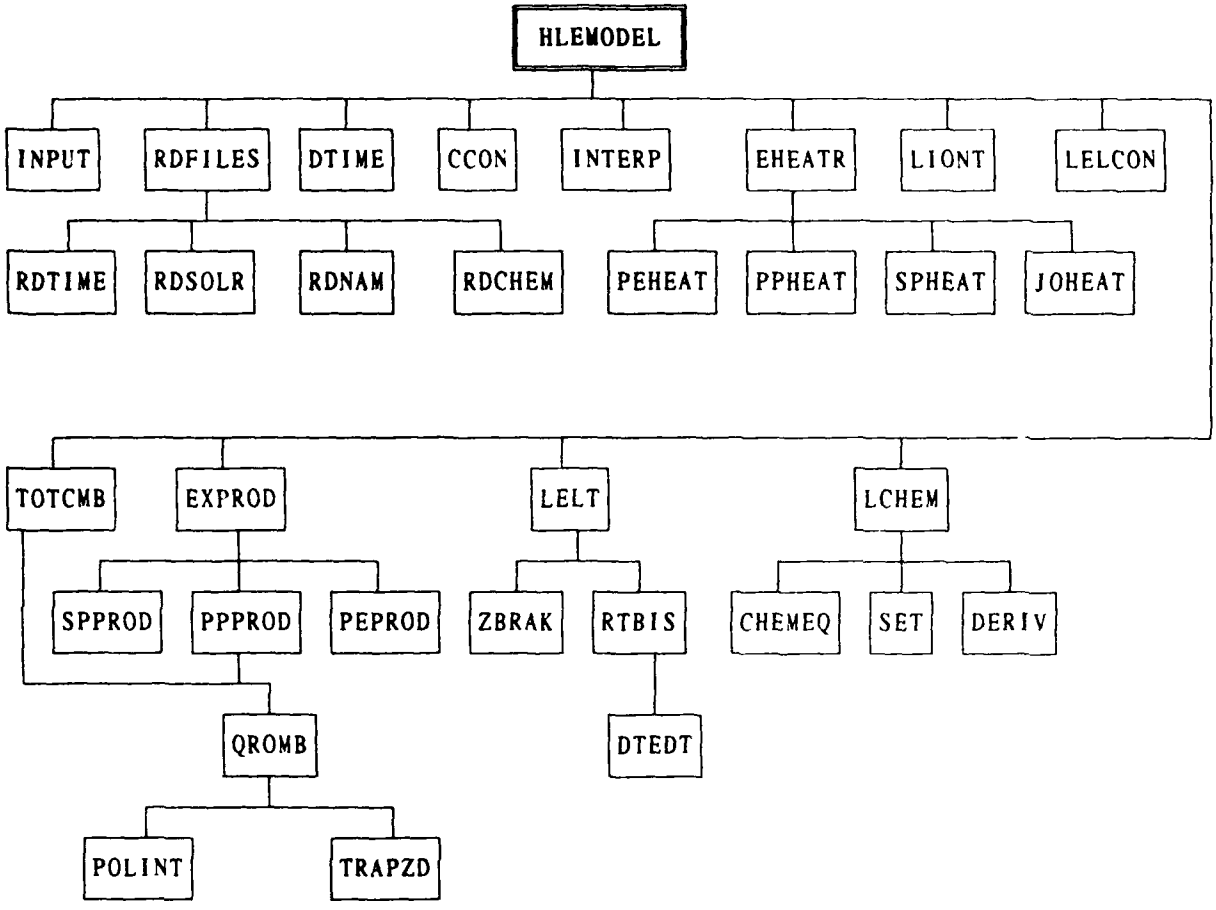
HLEMODEL
INPUT
RDFILES
DTIME
CCON
INTERP
EHEATR
LIONT
LELCON
RDTIME
RDSOLR
RDNAM
RDCHEM
PEHEAT
PPHEAT
SPHEAT
JOHEAT
TOTCMB
EXPROD
LELT
LCHEM
SPPROD
PPPROD
PEPROD
ZBRAK
RTBIS
CHEMEQ
SET
DERIV
QROMB
DTEDT
POLINT
TRAPZD

Section 5.2 Input and Output

All input files necessary for the execution of PRISM have been supplied with it. No additional user input is required if the supplied command file is used to execute the program.

Output consists of a single large file giving electron density profiles (EDP's) on a grid of 2° increments in latitude and 5° increments in longitude. The grid covers all latitudes (-90° to 90°) and longitudes (0° to 360°).

Section 5.3 Sample Results Using Simulated Data

We present one sample run of PRISM. A complete set of DISS, SSIES, and combined SSUSI and SSULI data for the midlatitude region was simulated using FAIM (the Fully Analytic Ionospheric Model). The sunspot number was set to 70 ($F_{10.7}$ = 120), and K_p was set to 5. High latitude data was actual data used in validating HLISM. We present here only the midlatitude results.

In Figures 3 and 4, we show contours of f_oF_2 and f_oE from FAIM. In Figures 5 and 6 we show contours of f_oF_2 and f_oE produced by PRISM based on the simulated data.

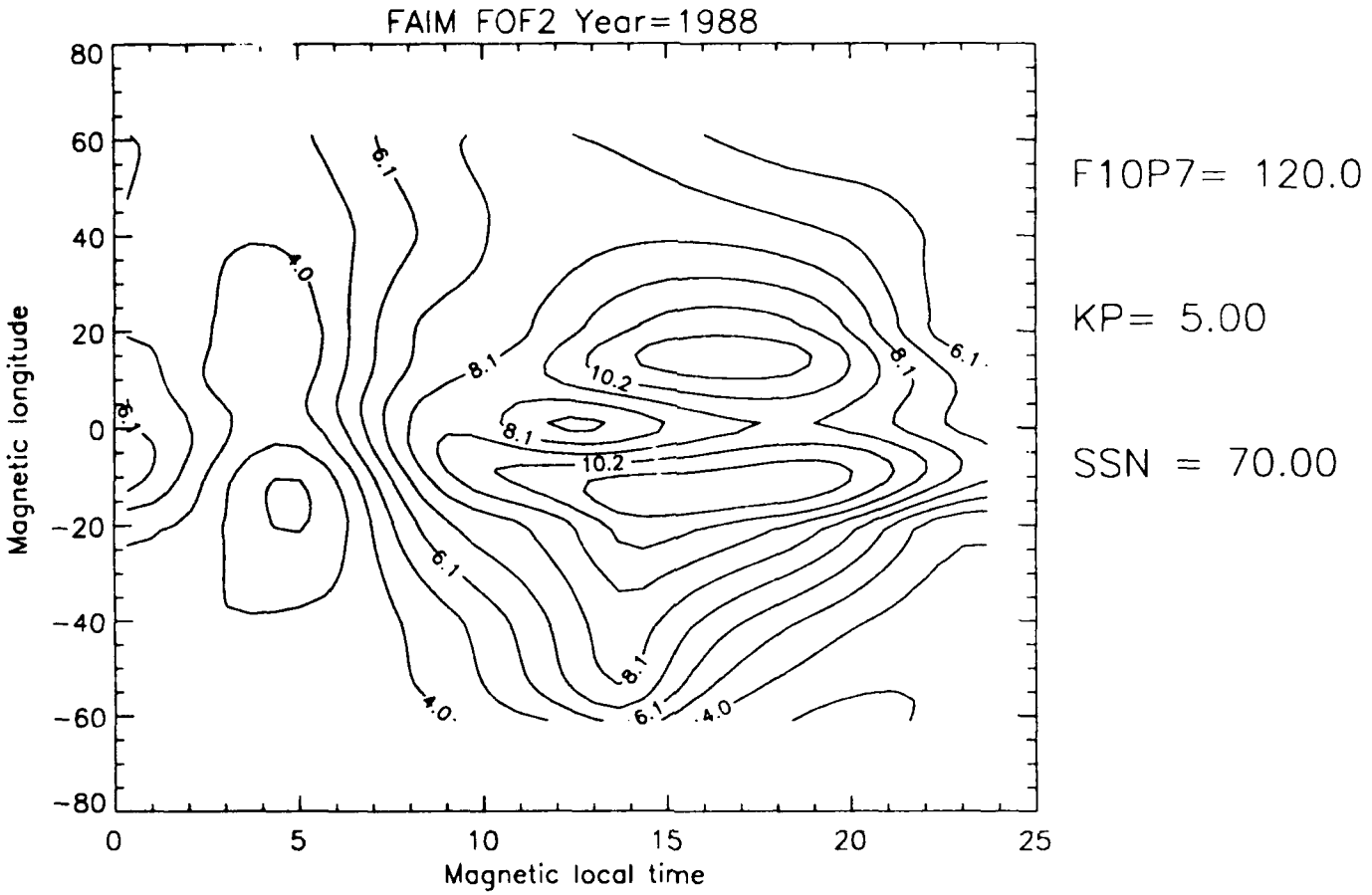

Contours at [1.9, 3.0,..., 11.2]

Figure 3 Contours of $f_o F_2$ from FAIM for 1800 UT on 22 April 1988 with a sunspot number of 70 ($F_{10.7}$ = 120) and a K_p of 5.

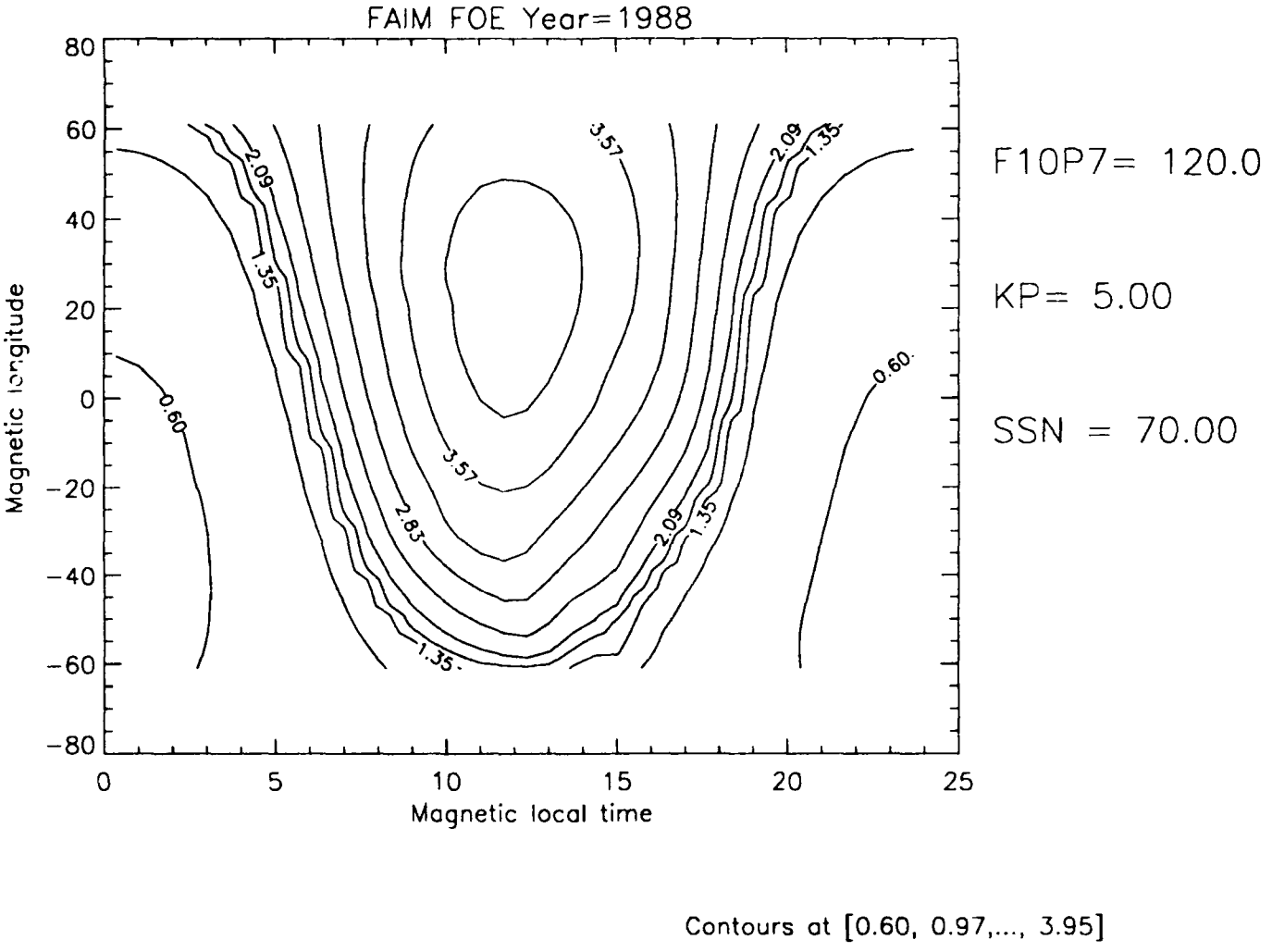

Figure 4 Contours of f_oE from FAIM for the same date and conditions as Figure 3

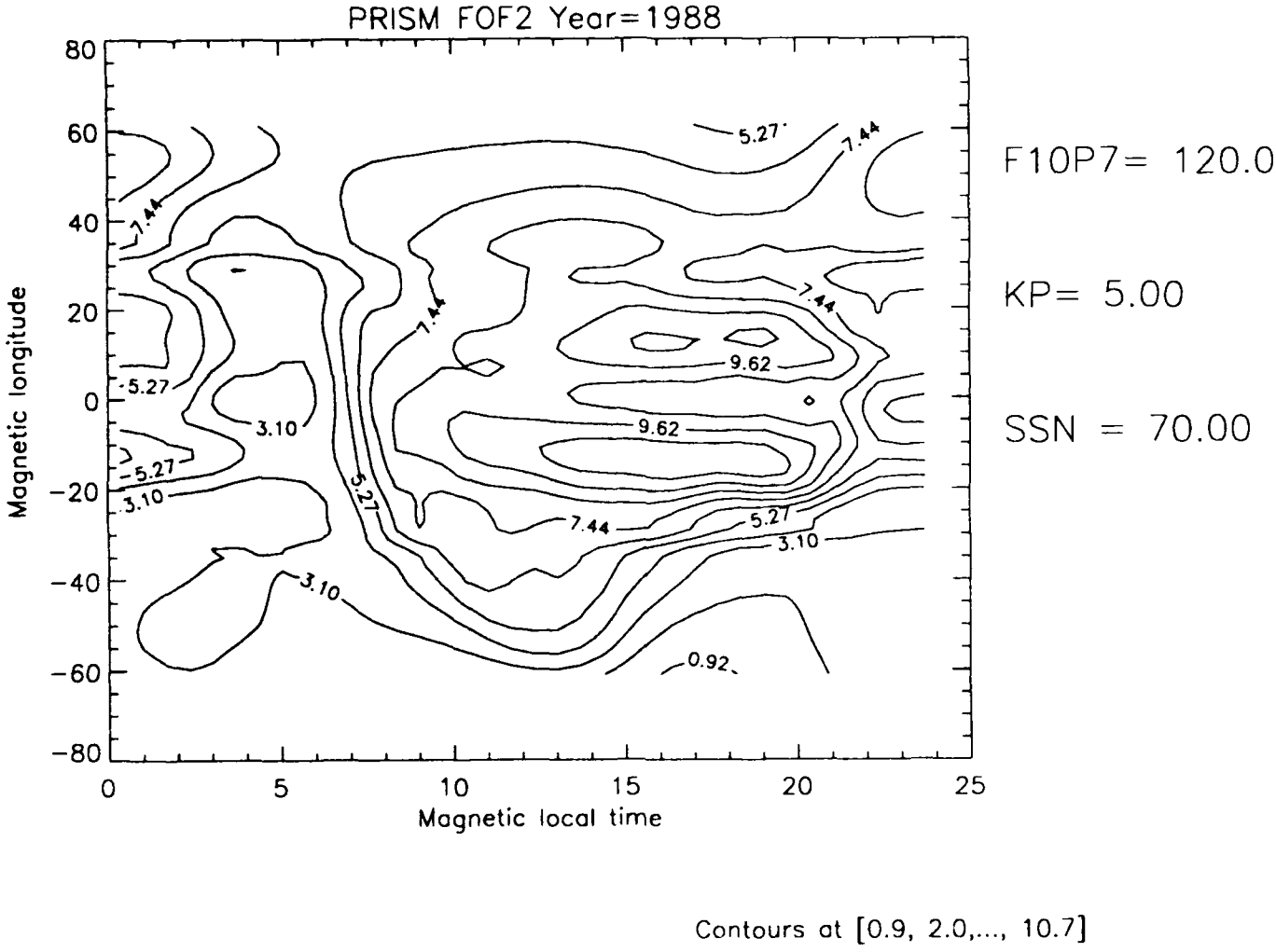

Figure 5 Contours of f_0F_2 produced by PRISM using input data simulated from FAIM for the date and conditions of Figure 3

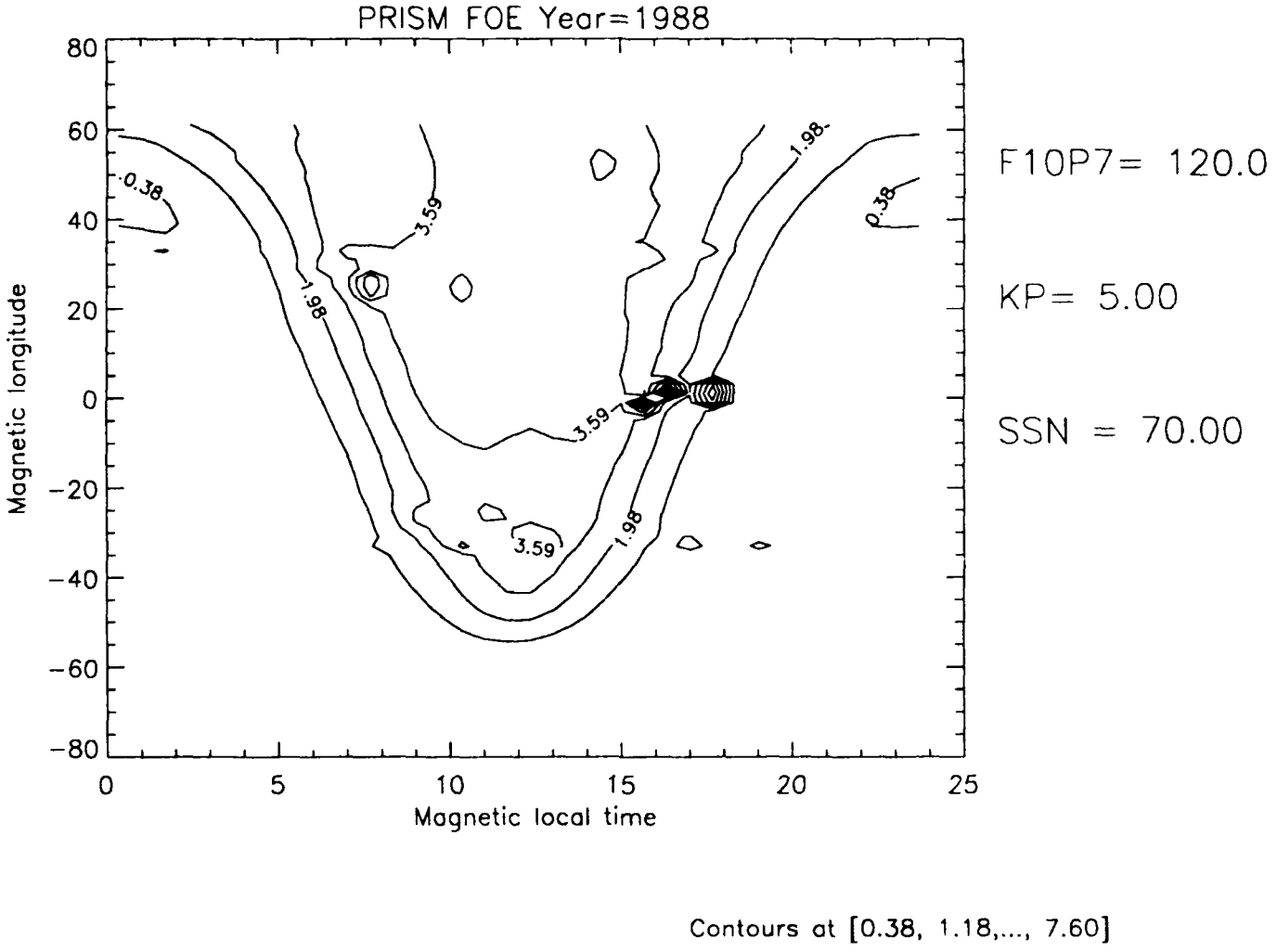

Figure 6 Contours of f_oE produced by PRISM using input data simulated by FAIM for the date and conditions of Figure 4

Section 6: References

Anderson, D. N., A theoretical study of the ionospheric *F*-region equatorial anomaly, II, Results in the American and Asian sectors, *Planet. Space. Sci.*, 21, 421-442, 1973.

Beckmann, P., Orthogonal Polynomials for Engineers and Physicists, The Golem Press. Boulder, pp. 91-92, 1973.

Brace, L. H., and R. F. Theis, Global empirical models of ionospheric electron temperature in the upper F-region and plasmasphere based on in situ measurements from the Atmosphere Explorer-C, ISIS 1, and ISIS 2 satellites, *J. Atmos. Terr. Phys.*, *43*, 1317, 1981.

Davis, R. E., Predictability of Sea Surface Temperature and Sea Level Pressure Anomalies Over the North Pacific Ocean, J. Phys. Oceanogr., 6, 249, 1976.

Fejer, B. G., The equatorial ionospheric electric fields, A review, *J. Atmos. Terr. Phys.*, *43*, 377-386, 1981.

Fejer, B. G., E. R. de Paula, I. S. Batista, E. Bonelli, and R. F. Woodman, Equatorial *F* region vertical plasma drifts during solar maxima, *J. Geophys. Res.*, *94*, 12049-12054, 1989.

Gussenhoven, M. S., D. A. Hardy, and N. Heinemann, Systematics of the equatorward diffuse auroral boundary, *J. Geophys. Res.*, *88*, 5692-5708, 1983.

Hardy, D. A., M. S. Gussenhoven, R. R. Raistrick, and W. J. McNeil, Statistical and functional representations of the pattern of auroral energy flux, number flux, and conductivity, *J. Geophys. Res.*, 92, 12275-12294, 1987.

Hedin, A. E., MSIS-86 Thermospheric Model, *J. Geophys. Res.*, 92, 4649-4662, 1987.

Hedin, A. E., Empirical global model of upper thermosphere winds based on Atmospheric and Dynamics Explorer satellite data, *J. Geophys. Res.*, *93*, 9959-9978, 1988.

Heppner, J. P., and N. C. Maynard, Empirical high-latitude electric field models, *J. Geophys. Res.*, *92*, 4467-4489, 1987.

Hildebrand, F. B., Methods of Applied Mathematics, Prentice-Hall, Englewood Cliffs, pp. 30-34, 1965.

Jasperse, J. R., The photoelectron distribution function in the terrestrial ionosphere, in *Physics of Space Plasmas*, ed. by T. S. Chang, B. Coppi, and J. R. Jasperse, Scientific Publishers, Cambridge, MA, pp. 53-84, 1982.

Kutzbach, J. E., Empirical Eigenvectors of Sea-Level Pressure, Surface Temperature, and Precipitation Complexes over North America, J. Appl. Meteor., 6, 791, 1967.

Lorenz, E. N., Empirical Orthogonal Functions and Statistical Weather Prediction, Sci. Rep. No. 1, Contract AF19(604)1566, AFCRC-TN-57-256, Dept. Meteor., MIT, 1956.

Moffett, R. J., The equatorial anomaly in the electron distribution of the terrestrial F-region, *Fundamentals of Cosmic Physics*, 4, 313-391, 1979.

Schunk, R. W., A Mathematical Model of the Middle and High Latitude Ionosphere, *Pageoph*, **127**, 255-303, 1988.

Secan, J. A., and T. F. Tascione, The 4D Ionospheric Objective Analysis Model, in Proceedings of the 1984 Ionospheric Effects Symposium, ed. by Goodman, Klobuchar, and Soicher, 336-345, 1984.

Strickland, D. J., D. L. Book, T. P. Coffey, and J. A. Fedder, Transport equation techniques for the deposition of auroral electrons, *J. Geophys. Res.*, 81, 2755-2764, 1976.

Strickland, D. J., B. Basu, J. R. Jasperse, and R. E. Daniell, A theory for the electron-proton-hydrogen atom aurora, to be submitted to *J. Geophys. Res.*, 1991.